Bioconjugate Chemistry

Article

pubs.acs.org/bc

Conjugation of a New Series of Dithiocarbazate Schiff Base Copper(II) Complexes with Vectors Selected to Enhance Antibacterial Activity

May Lee Low,[†,‡] Laure Maigre,[§] Pierre Dorlet,[∥] Régis Guillot,[⊥] Jean-Marie Pagès,[§] Karen A. Crouse,*[,‡] Clotilde Policar,*[,†] and Nicolas Delsuc*[,†]

[†]Laboratoire des BioMolécules, UMR 7203, CNRS, Université Pierre et Marie Curie, Ecole Normale Supérieure, Département de Chimie, 24 rue Lhomond, 75005 Paris, France

[‡]Department of Chemistry, Universiti Putra Malaysia, 43400 Serdang, Selangor, Malaysia

[§]UMR-MD1, Aix-Marseille Université, IRBA, 27 boulevard Jean Moulin, 13385 Marseille, France

[∥]Laboratoire Stress Oxydant et Détoxication, Institute for Integrative Biology of the Cell (I2BC), Université Paris-Saclay, CEA, CNRS, Bât 532 CEA Saclay, 91191 Gif sur Yvette cedex, France

[⊥]Institut de Chimie Moléculaire et des Matériaux d'Orsay, Université Paris-Sud Bât. 420, 91405 Orsay, France

Supporting Information

ABSTRACT: A new series of six Schiff bases derived from S-methyldithiocarbazate (SMDTC) and S-benzyldithiocarbazate (SBDTC) with methyl levulinate (SMML, SBML), levulinic acid (SMLA, SBLA), and 4-carboxybenzaldehyde (SM4CB, SB4CB) were reacted with copper(II), producing complexes of general formula ML_2 (M = Cu(II), L = ligand). All compounds were characterized using established physicochemical and spectroscopic methods. Crystal structures were determined for three Schiff bases (SMML, SBML, SBLA) and two Cu(II) complexes ($Cu(SMML)_2$ and $Cu(SMLA)_2$). In order to provide more insight into the behavior of the complexes in solution, electron paramagnetic resonance (EPR) and electrochemical experiments were performed. The parent ligands and their respective copper(II) complexes exhibited moderate antibacterial activity against both Gram-negative and Gram-positive bacteria. The most active ligand (SB4CB) and its analogous S-methyl derivative (SM4CB) were conjugated with various vector moieties: polyarginines (R1, R4, R9, and RW9), oligoethylene glycol (OEG), and an efflux pump blocker, phenylalanine-arginine-β-naphthylamide (PAβN). Nonaarginine (R9) derivatives showed the most encouraging synergistic effects upon conjugation and complexation with copper ion including enhanced water solubility, bacteria cell membrane permeability, and bioactivity. These Cu(II)-R9 derivatives display remarkable antibacterial activity against a wide spectrum of bacteria and, in particular, are highly efficacious against *Staphylococcus aureus* with minimum inhibitory concentration (MIC) values of 0.5−1 μM. This pioneer study clearly indicates that the conjugation of cell-penetrating peptides (CPPs) to dithiocarbazate compounds greatly enhances their therapeutic potential.

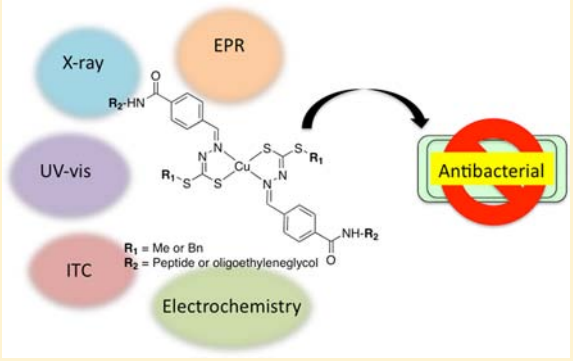

INTRODUCTION

The challenge of multidrug resistance (MDR) has become a critical issue in treating bacterial infections. The continuous dissemination of MDR bacteria drastically reduces the efficiency of the antibiotic arsenal and consequently increases the frequency of therapeutic failure.[1,2] Therefore, there is an urgent need to develop new drugs with novel mechanisms of action and higher activity to address the MDR challenge. In view of this, Schiff bases derived from S-alkyl/aryl esters of dithiocarbazic acid and their coordination complexes, with their abundance of potentially exciting biological activities that can be readily modulated by introducing different substituents, are attractive candidates for consideration.[3−7] In many cases, the bioactivities of these dithiocarbazate derivatives differ widely although they vary only slightly in molecular structure.[3−7]

Copper complexes represent a class of compounds that have been subjected to intensive research because of their potential therapeutic applications[8] particularly as antitumor[9,10] and antibacterial agents.[11,12] A number of thiosemicarbazone copper complexes have been found to be active in cell destruction, as well as in the inhibition of DNA synthesis.[13,14] Recently, Cu(II) complexes of tetradentate (NNSS) thiosemicarbazone ligands have been extensively explored as radiopharmaceuticals for the specific targeting of hypoxic tissue.[15] They are known to be stable ($K_{ass} = 10^{18}$) and neutral and they can easily cross cellular membranes.[15,16] Copper is therefore an excellent choice in the continuing search for new and effective metallodrugs. However, as most sulfur−nitrogen chelating

Received: October 27, 2014
Published: November 10, 2014

   dx.doi.org/10.1021/bc5004907 | *Bioconjugate Chem.* 2014, 25, 2269−2284

ligands and their copper complexes are hydrophobic,[17,18] their consequential low solubility in water imposes experimental limitations in biological studies; the introduction of a functional group to increase their solubility could potentially enhance their delivery and expand their applications. In addition, the design of therapeutic agents that efficiently pass into cells remains a major challenge.[19] Many drug candidates and probe molecules fail due to undesirable side effects resulting from high quantities of material administered necessitated by low cell uptake.[20] It is therefore critical to optimize cellular uptake to develop potent and selective metal complexes as chemotherapeutic or diagnostic agents.

In the present work, the biological potential of Schiff bases and their respective open chain Cu(II) complexes (CuL_2) derived from S-methyl or S-benzyldithiocarbazate with methyl levulinate (SMML, SBML), levulinic acid (SMLA, SBLA), and 4-carboxybenzaldehyde (SM4CB, SB4CB) was explored by determining their potency against different bacterial strains expressing a multidrug resistant phenotype. The most biologically active and stable ligands selected from the initial stage of this study were further optimized by functionalizing them with various vectors using either standard solid-phase peptide synthesis (SPSS) or synthesis in solution. Symmetrical coordination of two ligands to Cu(II) produced complexes containing two functionalizing groups. Related work in the literature on bis(thiosemicarbazone) used for radiopharmaceutical purposes reported complexes containing only a single tetradentate targeting agent. It is possible that the presence of additional functional groups could be counterproductive due to compromised pharmacokinetics[21] or could lead to better biological properties as highlighted by Ma et al.[22,23]

In attempting to improve delivery, a complex with an oligoethylene glycol (OEG) moiety was prepared. Being a neutral water solubilizing agent that does not show any antimicrobial activity,[24,25] OEG is expected to improve the bioactivity only by enhancing water solubility of the complex. Also, since the presence of dimeric cell-penetrating peptides (CPPs) has been shown to dramatically improve the capacity of ligands[26] and Pt complexes[27] to enter various cells, compounds conjugated with CPPs, also called "Trojan horse peptides",[28,29] were studied. Their unique ability to cross the plasma membrane and internalize in cells make them very powerful tools for the transportation of a great variety of substances ranging from small therapeutic drugs to large proteins and DNA.[19] The lower toxicity and controlled administration of CPPs provide several advantages for their use as molecular vehicles.[30] For polyarginine CPPs, cell uptake is known to be optimum for peptides with 8 to 15 arginine residues.[31] Since the preparation of the complexes in this study involved 2 equiv of ligands, onto each of which a peptide was to be attached, different peptide chains with lengths of one (R1) or four (R4) arginines were introduced in addition to R9, a commonly used CPP, to determine their influence. Additionally, since some CPPs and antimicrobial peptides (AMPs) are known to share several common characteristics such as high density in basic residues and an amphipathic secondary structure in membrane environments,[32] it is understandable that conjugation of metal binding ligands with AMPs would significantly enhance the permeability and activity of the compounds against bacteria that have developed cross-resistance.[33,34] Having considered that these bioactive peptide sequences consist mainly of arginine and tryptophan, RW9 (a peptide derived from penetratin) was chosen as a good candidate for bioconjugation.[35] Finally, knowing that one resistance pathway of multidrug-resistant bacteria involves the overexpression of efflux pumps, which expel structurally unrelated antibiotics, thus decreasing their intracellular concentration,[36−38] C-capped dipeptide, phenylalanine-arginine-β-naphthylamide (PAβN), a blocker of efflux pumps,[37] was grafted to the ligand to gain an understanding of efflux-mediated resistance in selected bacterial pathogens. Investigation of the action of efflux pumps was performed using pump-deleted strains. In this investigation, PAβN was directly linked to the potential antibacterial agent, namely, the ligand and Cu(II) complex, in order to reveal any synergistic effect that could possibly challenge the efficiency of efflux pump.

Although many dithiocarbazate derivatives have been reported in the literature, there are few reports linking their bioactivity with crystallography, EPR, and/or electrochemistry.[39−41] It is essential that efforts be directed toward correlating the bioactivity of this class of compounds with both their solid and solution structures as well as their redox properties. The results from such investigations will enable rational design of compounds to lead to a better understanding of their mechanism of action.

RESULTS AND DISCUSSION

Cu(II) Complexes with Bidentate NS Ligands Possessing an Acid or Ester Functionality. *Synthesis.* S-substituted dithiocarbazates (SBDTC and SMDTC) were first prepared as previously described.[44,45] Then, six bidentate Schiff bases were prepared via the condensation reaction between the respective S-substituted dithiocarbazates and carbonyl compounds in equimolar amounts (Scheme 1).

Scheme 1. Synthesis of the Copper Complexes Derived from Bidentate Dithiocarbazate Ligands[a]

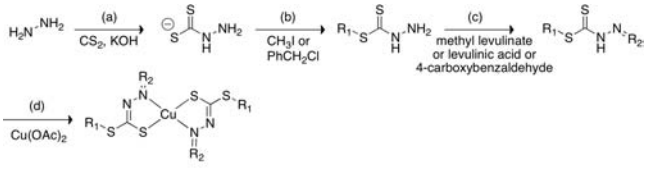

Entry	Name	R_1	R_2
1	SMML	$-CH_3$	$=C(CH_3)-CH_2-CH_2-COOCH_3$
2	SMLA	$-CH_3$	$=C(CH_3)-CH_2-CH_2-COOH$
3	SM4CB	$-CH_3$	$=C(H)-C_6H_4-COOH$
4	SBML	$-CH_2Ph$	$=C(CH_3)-CH_2-CH_2-COOCH_3$
5	SBLA	$-CH_2Ph$	$=C(CH_3)-CH_2-CH_2-COOH$
6	SB4CB	$-CH_2Ph$	$=C(H)-C_6H_4-COOH$

[a](a) EtOH, 0 °C, 1 h; (b) EtOH, 0 °C, 5 h; (c) for SMML and SBML (methyl levulinate, EtOH, 79 °C, 1 h), for SMLA and SBLA (levulininc acid, acetonitrile, 82 °C, 1 h), for SM4CB and SB4CB (4-carboxybenzaldehyde, acetonitrile, 82 °C, 2 h); (d) For $Cu(SMML)_2$ and $Cu(SMLA)_2$ (MeOH, r.t., overnight), for $Cu(SBML)_2$ and $Cu(SBLA)_2$ (toluene, r.t., overnight), for $Cu(SM4CB)_2$ and $Cu(SB4CB)_2$ (acetonitrile, 82 °C, 2 h).

Reactions with methyl levulinate were carried out in ethanolic solution at 79 °C whereas those involving both levulinic acid and 4-carboxybenzaldehyde containing the acid −COOH functionality were done in hot acetonitrile to avoid esterification. Depending on the ligands, different reaction conditions were chosen to optimize the yield and purity of the

dx.doi.org/10.1021/bc5004907 | Bioconjugate Chem. 2014, 25, 2269−2284

complexes. The proposed CuL_2 structure in which the ligands are bidentate was initially established by elemental analysis and mass spectrometry. All the mass spectra show signals corresponding to the molecular weight of either the protonated complexes or the complexes with sodium or potassium counterions confirming 1:2 metal to ligand stoichiometry. The purity of the compounds and their stability in aqueous medium were evaluated using RP-HPLC on a C8 column. The compounds were eluted with an increasing percentage of ACN in H_2O (5% to 100% ACN) over 30 min with both solvents containing 0.1% TFA to maintain the pH. For the aliphatic ester and acid Schiff bases (SMML, SMLA, SBML, SBLA), the chromatograms of the ligands showed two peaks corresponding to the starting S-substituted dithiocarbazate and the expected ligand, whereas the complexes showed mainly a single peak corresponding to the copper complexes (see Supporting Information 5.1). Another tiny peak visible for the Cu(II) complexes may be due either to isomerization or to dissociation to 1:1 Cu:L complexes. The aromatic acid Schiff bases (SM4CB and SB4CB) on the other hand showed only a single peak corresponding to the ligands, evidence of their enhanced stability as compared to their aliphatic counterparts under these conditions. These observations indicate that the -C═N- hydrazone bond in the aliphatic free ligands could be hydrolyzed in acidic conditions, but complexation significantly increased stability and aromatic Schiff bases were clearly more stable than their aliphatic analogues. The difference in stability of the ligands and metal complexes indicates that metal complexation can possibly be used to protect the ligand from degradation before it reaches its target in biological systems. Upon complexation of metal ion, deprotonation of the dithiocarbazate nitrogen leading to an iminothiolate is expected. Coordination via NS atoms is anticipated while the O atom in ligands containing an acid or ester moiety also has the potential to participate in metal coordination. In order to confirm the formation of the expected metal complexes and to better characterize them, additional techniques were employed.

Characterization of Nonconjugated Compounds in Solid State. The FT-IR spectra of the SMML and SBML ligands exhibit characteristic bands νNH at ca. 3200 cm^{-1}. The spectra of the ligands containing the acid functionality, SMLA, SBLA, SM4CB, and SB4CB, displayed strong broad bands spanning 3300−2300 cm^{-1} due to overlapping ν(OH), ν(NH), and ν(CH) stretching. Upon formation of the complexes, the band corresponding to the ν(NH) stretching of the ligands disappeared suggesting that the nitrogen atom was deprotonated during coordination with the Cu(II) ion. In addition, the strong band assigned to the azomethine ν(C═N) vibration observed between 1652 and 1611 cm^{-1} in the spectra of the ligands experienced a downward shift of ca. 5−40 cm^{-1} indicating coordination of the ligands to the Cu(II) ion via the azomethine nitrogen atoms. The hydrazinic ν(N−N) band between 834 and 778 cm^{-1} also shifted either to higher or lower wavenumbers upon metal complexation further supporting nitrogen atom coordination. The disappearance of ν(C═S) at ca. 1067−1025 cm^{-1} and the splitting of asymmetric ν(CSS) of the free ligand at ca. 990−923 cm^{-1} in the spectra of the Cu(II) complexes were strong evidence of coordination via the thiolate sulfur atoms.[46,47] It is also interesting to note that a second band due to ν(N═C) in complexes containing anionic dithiocarbazate moieties was also resolved[48] for $Cu(SBLA)_2$. Finally, in the spectra of $Cu(SM4CB)_2$, $Cu(SB4CB)_2$, and $Cu(SBLA)_2$, the strong band at 1717−1687 cm^{-1} assigned to ν(C═O) remained unchanged, indicating that this oxygen is not coordinated. However, for $Cu(SMML)_2$, $Cu(SBML)_2$, and $Cu(SMLA)_2$, this band shifted slightly (9−14 cm^{-1}). This discrepancy was resolved by single crystal X-ray analysis discussed below. The Cu(II) ions in $Cu(SMML)_2$, and $Cu(SMLA)_2$ were determined to be coordinated to only the azomethine nitrogen and thiolate sulfur atoms. Observation of intermolecular hydrogen bonds involving the carbonylic oxygen and the presence of other short contacts in the X-ray structures of the ligands and complexes (see Supporting Information 5.3) suggest that the ν(C═O) shift in the spectra of $Cu(SMML)_2$ and $Cu(SMLA)_2$ must be the result of vibrational coupling of the C═O in the H-bonded structure in the solid state.[49,50] ORTEP diagrams for SMML, SBLA, SBML, and for $(CuSMML)_2$ and $(CuSMLA)_2$ are shown in Figures 1 and 2, respectively.

SBML crystallized in space group of $P2_1/n$ whereas SMML and SBLA crystallized in space groups $P2_1/c$ and $P\bar{1}$, respectively. The Schiff bases are in the thione form with C═S bond distances ranging from 1.6617(11) to 1.682(3) Å. The bond lengths were intermediate between a C−S single bond and a C═S double bond possibly due to the extensive conjugation over the C═N−N−C chain and other intermolecular interactions.[51,52] The N−N bond distance varied from 1.3797(7) to 1.3941(13) Å in the Schiff bases, showing that the bond was shorter than a single bond, also indicating significant π-delocalization along the dithiocarbazate moiety.[51−53] *Trans*−*cis* isomerism was exhibited in all the Schiff bases around the -SC(═S)NH- moiety. It was observed that the methyl levulinate/levulinic acid chain was *trans* with respect to the terminal thione S atom about the C−N bond while the S-methyl/S-benzyl group was *cis* with respect to the terminal thione S atom about the C−S bond. The bond angles in the Schiff bases were close to 120° consistent with sp^2 hybridization. The Schiff bases are not planar since both the benzyl rings and the methyl levulinate/levulinic acid moieties are in a twisted conformation as shown by their dihedral angles. The benzyl ring in the S-benzyl derivatives was almost perpendicular to the dithiocarbazate plane. The N−N(H)−C═S and N(H)−C−S−C(benzyl/methyl) chains adopted *trans* conformation with torsion angles of ca. (±)178°, whereas the S═C−S−C (benzyl/methyl) chain adopted *cis* conformation with torsion angle from −2.10(9) to 4.4(3)°. The configuration about the C═N double bond was *E* (torsion angle $C(H_2)$−C═N−N(H) = ca. (±)179°).

$Cu(SMML)_2$ crystallized in the $C2/c$ space group as a centrosymmetric complex in which the two ligands were symmetrically related to each other and have the same bond angles and distances. The central copper ion was bis-chelated by the uninegatively charged bidentate ligand through the azomethine nitrogen atoms (N2) and thiolate sulfur atoms (S1) as shown in Figure 2. The sum of the four angles, N−Cu−S, S−Cu−S, S−Cu−N, and N−Cu−N, in the complex was 374.31° confirming a square planar geometry about the copper ions with significant distortion.[54] Neither the carbonylic nor hydroxylic oxygen of the methyl levulinate moiety participated in complexation. The conjugation system of the moieties was influenced by coordination with the metal as shown by slight lengthening of the N1−N2 bond distance (1.4066(12) Å). In addition, the azomethine C2−N1 bond in the complex (1.2958(14) Å) was shorter than in the ligand (1.3427(7) Å) and typical for a double bond, which clearly indicates that complexation involves deprotonation at N1. Indeed, the C−S

dx.doi.org/10.1021/bc5004907 | *Bioconjugate Chem.* 2014, 25, 2269−2284

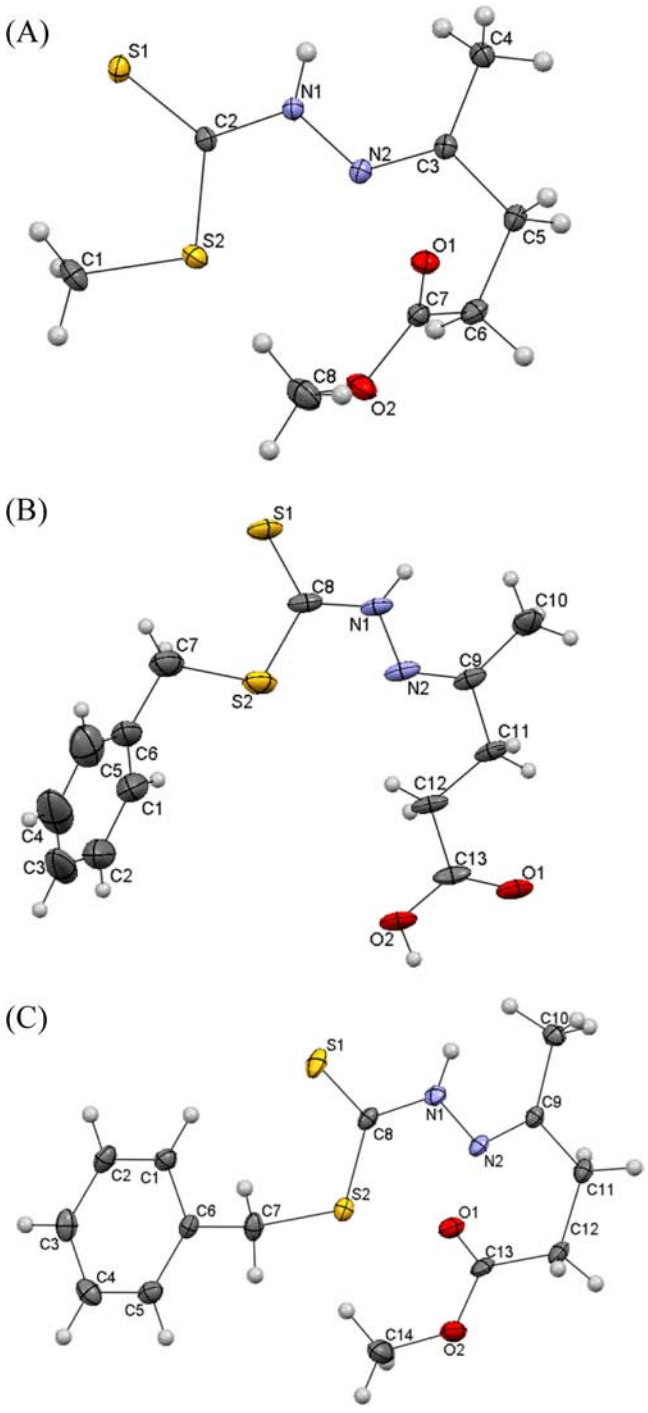

Figure 1. ORTEP diagrams of (A) SMML, (B) SBLA, and (C) SBML. Ellipsoids are drawn at the 50% probability level.

bond was also strongly affected. The C2−S1 bond length in the complex was longer (1.7367(1) Å) than that observed in the Schiff base, SMML, indicating single bond character as expected when complexation involves the ligand in its thiol form.

$Cu(SMLA)_2$ crystallized in $P2_1/n$ space group within an asymmetric unit in which two nonequivalent ligand molecules were present with one methanol molecule. Similar to $Cu(SMML)_2$, deprotonation of the ligand lead to tautomerization to the iminothiolate. While coordinating in the iminothiolate form, the negative charge generated on the sulfur atom was delocalized in the C═N−N═C chain as indicated

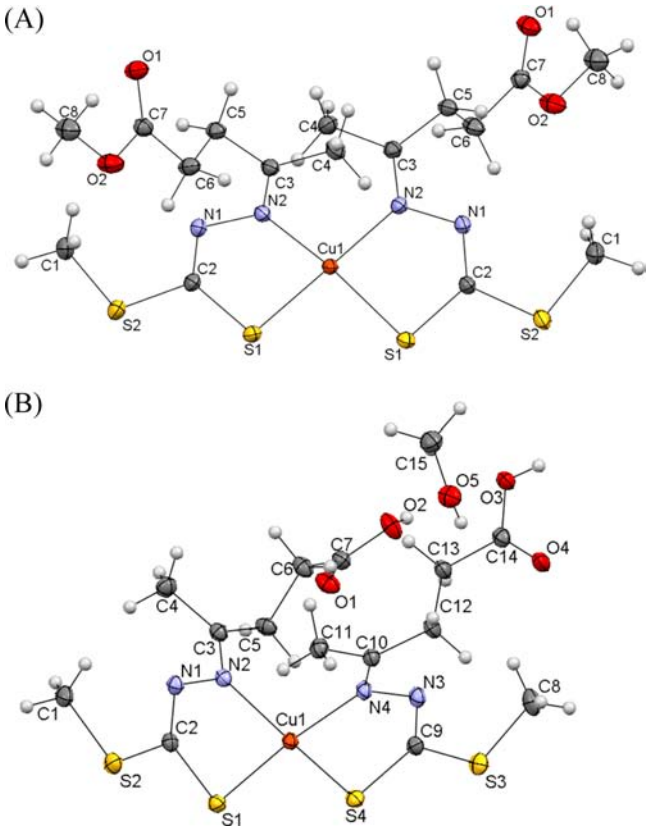

Figure 2. ORTEP diagrams of (A) $Cu(SMML)_2$ and (B) $Cu(SMLA)_2$. Ellipsoids are drawn at the 50% probability level.

by the intermediate C2−N1 = 1.2999(2) and 1.2861(3) Å, N1−N2 = 1.410(2) Å, and N2−C3 = 1.287(2) Å bond lengths. The lengthening of the C−S bond in the complex can be attributed to enethiolization. The 380.12° sum of angles around the Cu(II) ion in $Cu(SMLA)_2$ indicated that the complex was more distorted from regular square-planar geometry than $Cu(SMML)_2$. The Cu−S (2.2356(5) and 2.2287(5) Å) and Cu−N (1.9898(16) and 1.9912(16) Å) bond lengths are similar to those of the bis-chelated four coordinate Cu(II) complex of the related isatin Schiff base of SMDTC.[55,56] The differences between the bond lengths in the same complex can be ascribed to the constraints imposed by chelation.

Characterization of Nonconjugated Compounds in Solution. In order to investigate the formation of complexes in solution, UV−vis spectra of all metal complexes were recorded at concentrations between 25 μM and 1 mM. The electronic spectra of the Schiff bases showed two bands, between 273 and 364 nm, arising from $\pi \rightarrow \pi^*$ and n $\rightarrow \pi^*$ transitions. For all metal complexes, the first band corresponding to the $\pi \rightarrow \pi^*$ (256−300 nm) transition is always observed, whereas the second intraligand band at higher wavelength (300−400 nm) ascribed to n $\rightarrow \pi^*$ band either showed a blue shift with a reduction of intensity or it disappeared. This is due to donation of the lone pair of electrons to the metal and hence the coordination of the azomethine group.[57] Most Cu(II) complexes in this work showed the presence of ligand-to-metal charge transfer (LMCT) bands (400−450 nm) arising from S → M(II) interaction.[46] The d^9 Cu(II) complexes also displayed a broad d−d band at ca. 604 nm due to Jahn−Teller distortion from square planar geometry.[58] Examples of the UV−vis spectra for $Cu(SMML)_2$ and SMML are shown in Figure 3.

dx.doi.org/10.1021/bc5004907 | *Bioconjugate Chem.* 2014, 25, 2269−2284

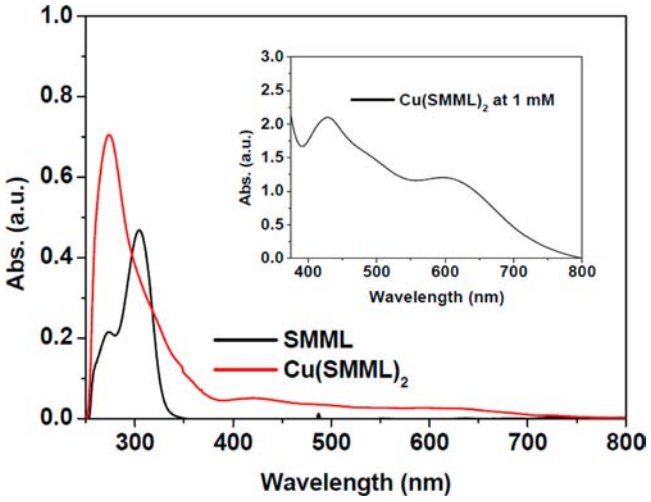

Figure 3. UV−vis spectra recorded for SMML and $Cu(SMML)_2$ at 25 μM. Inset shows d−d band of the complex at 1 mM.

The Cu(II) complexes of 4-carboxybenzaldehyde, $Cu(SM4CB)_2$ and $Cu(SB4CB)_2$, however, showed neither the sulfur-to-copper LMCT band at 400 nm nor the d−d band. The absence of these bands even at high concentration (1 mM) suggests that the ligand does not have a suitable low-lying antibonding π^* orbital.[59] These two complexes showed a broad band spanning 300−400 nm with λ max at ∼328 nm.

To ascertain the formation of the Cu(II) complexes with the proposed 1:2 metal to ligand stoichiometry, titration experiments were performed in DMSO and in acetate buffer (see Supporting Information 5.6). Upon addition of $Cu(OAc)_2$, changes in the UV−vis spectra were obvious with the intensity of the intraligand band at λ_{max} ∼340 nm decreasing until the signature broad band spanning 300−400 nm was observed when the complex formed. Complexation proceeded with a sharp end-point at 0.5 equiv with clear isosbestic points indicative of a single complexation event with 1:2 metal to ligand stoichiometry. The stoichiometry of the complex was further confirmed by isothermal titration calorimetry (ITC). The titration performed with SB4CB showed that $Cu(SB4CB)_2$ complex formation was entropically driven due to the chelate effect. The association constant, log K_{ass}, was 5.56.

In order to gain insight into the structure of the complexes in solution, their EPR spectra were recorded in DMF (examples of EPR spectra are shown in Figure 4). The EPR parameters are summarized in Table 1. Spectra of frozen solutions of all bidentate Schiff base Cu(II) complexes in DMF showed evidence of two species, one being present in a relatively minute amount. The spectra of the main species included well-resolved axial Cu(II) signals having significant separation of $g_\perp$ and $g_{//}$ with hyperfine splitting at $g_{//}$. The observation that $g_{//} > g_\perp$ is typical of axially symmetric mononuclear d^9 Cu(II) complexes in a ground state doublet with the unpaired electron residing in a $dx^2 - y^2$ orbital while the $g_{//} < 2.3$ revealed that the metal−ligand bond was predominantly covalent in character.[60,61] The g and A parameters indicated that the metal coordination environment involved two nitrogen atoms in a distorted square-planar geometry for the aliphatic acid and ester Schiff base Cu(II) complexes. The empirical factor f ($=g_{//}/A_{//}$) values for $Cu(SMML)_2$, $Cu(SMLA)_2$, $Cu(SBML)_2$, and $Cu(SBLA)_2$ were very close to one another and confirmed deviation of their geometry from square-planar.[12,62,63] However, there were also differences in this series in which the f values for aromatic acid derivatives $Cu(SM4CB)_2$ and $Cu(SB4CB)_2$ of 128 and 121 cm, respectively, are within the perfect range (105−135 cm) for square planar compounds. Finally, the calculated molecular orbital coefficients, α^2, between 0.61 and 0.70 indicated that these copper complexes have some covalent character, as suggested above.[48,64]

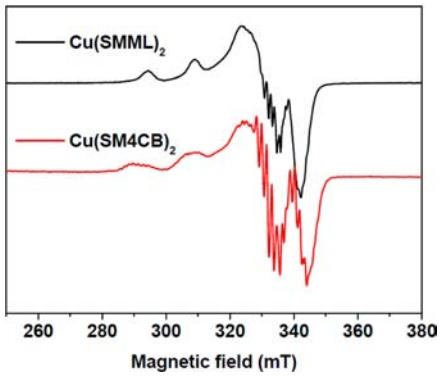

Figure 4. EPR spectrum of $Cu(SMML)_2$ and $Cu(SM4CB)_2$ at 1 mM in frozen DMF. Microwave frequency = 9.50 GHz, microwave power = 1.00 mW, modulation amplitude = 0.5 mT, modulation frequency = 100 kHz, time constant = 164 ms, temperature = 50 K.

Table 1. EPR Parameters Measured from the Spectra of the Copper(II) Complexes

compound	$g_{//}$	$g_\perp$	$A_{//}{}^a$	f^b	α^2
$Cu(SMML)_2$	2.15	2.05	438 (146)	147	0.61
$Cu(SMLA)_2$	2.15	2.06	438 (146)	147	0.62
$Cu(SBML)_2$	2.15	2.05	438 (146)	147	0.61
$Cu(SBLA)_2$	2.15	2.05	443 (148)	145	0.61
$Cu(SM4CB)_2$	2.15	2.05	504 (168)	128	0.67
$Cu(SB4CB)_2$	2.15	2.05	531 (177)	121	0.70

[a]Unit in MHz, in bracket = $A_\parallel \times 10^{-4}$ cm^{-1}. [b]Unit in cm.

The spectra in DMF for all Cu(II) parent complexes in this work show the presence of an additional minor component. This observation could suggest that two isomers or complexes with slightly different geometries are formed. Either *transoid* or *cisoid* ligand conformations with respect to the central metal-coordinated rings are possible for complexes in an open chain system since they are relatively labile.[65−67]

The $g_{//}$ region of the minor species for compounds $Cu(SMML)_2$, $Cu(SBML)_2$, $Cu(SMLA)_2$, and $Cu(SBLA)_2$ shifted downfield whereas it shifted upfield for $Cu(SM4CB)_2$ and $Cu(SB4CB)_2$ relative to the dominant species. The X-ray structures of $Cu(SMML)_2$ and $Cu(SMLA)_2$ show that the ligands adopt a *cisoid* orientation. Although there is no evidence to make a definitive assignment of the *transoid* and the *cisoid* species in solution, it can be argued that the predominant orientation in the solid may be indicative of an energetically preferred state. Thus, this may serve as a preliminary indication that the *cisoid* orientation is more favorable in aliphatic Cu(II) complexes and can be tentatively assigned to the major component. The difference observed in aromatic acids $Cu(SM4CB)_2$ and $Cu(SB4CB)_2$ could point toward both compounds having preference for the *transoid* conformation since the *cisoid* structure would result in increased steric hindrance especially with the presence of the aromatic ring. This ordering of the structures is also consistent with the interpretation of EPR results that the mainly *transoid*

dx.doi.org/10.1021/bc5004907 | Bioconjugate Chem. 2014, 25, 2269−2284

$Cu(SM4CB)_2$ and $Cu(SB4CB)_2$ were more planar compared to their aliphatic counterparts as indicated by the f values. This proposal is also in agreement with the LC-MS results for the aromatic acid Cu(II)-bioconjugates that showed two peaks having the same mass (see Supporting Information 5.5).

In order to gain a better understanding of the influence of different functional groups upon the electronic properties of coordinated metal centers, cyclic voltammetry (CV) measurements were performed with the various CuL_2 complexes at 0.0017 M in DMF containing 0.1 M tetrabutylammonium perchlorate as supporting electrolyte. All complexes displayed qualitatively similar redox behavior, yet the characteristic one-electron Cu(II)/Cu(I) quasi-reversible reduction waves shifted depending on the ligand (Table 2). The measured reduction potentials clearly correlate with the electron-donating ability of the functional group forming the Schiff bases and the S-substituted dithiocarbazate: the S-methyl derivatives showed lower Cu(II)/Cu(I) reduction potentials (E_{pc} = −92 to −114 mV) than the S-benzyl derivatives (E_{pc} = −66 to −79 mV). The reduction potentials can be arranged (toward the more negative) in the following order $Cu(SMML)_2$ < $Cu(SMLA)_2$ < $Cu(SM4CB)_2$. All compounds showed a similar trend when the cyclic voltammograms were recorded at different scan rates. For example, in the case of $Cu(SMML)_2$ (Figure 5), the peak current ratios of the anodic signal and the cathodic signal (i_{pa}/i_{pc}) remain close to 1 (see Supporting Information 5.8) independent of the sweep rate used indicating the reversibility and stability of the electrochemically generated product.[68]

Table 2. Electrochemical Data for the Cu(II) Complexes vs Ag/AgCl at 0.1 V

	Cu(II)/Cu(I)					Cu(II)/Cu(III)
compound	E_{pa} [mV]	E_{pc} [mV]	ΔE_p [a] [mV]	$\Delta E_{1/2}$ [b] [mV]	i_{pa}/i_{pc}	E_{pa} [V]
$Cu(SMML)_2$	2	−92	94	−45	1.00	1.000
$Cu(SMLA)_2$	−14	−95	81	−55	0.60	0.998
$Cu(SM4CB)_2$	−11	−114	103	−63	1.11	1.006
$Cu(SBML)_2$	21	−66	87	−23	1.01	1.001
$Cu(SBLA)_2$	8	−78	86	−35	0.84	0.985
$Cu(SB4CB)_2$	15	−79	94	−32	0.88	1.029

[a] $\Delta E_p = E_{pa} - E_{pc}$. [b] $\Delta E_{1/2} = 0.5(E_{pa} + E_{pc})$.

Furthermore, a linear correlation exists between the peak current and the square root of the scan rate. However, the voltammetric data shows that at higher scan rates, the reduction (E_{pc}) and oxidation (E_{pa}) peaks are shifted to more negative and positive values, respectively. The separation between them, ΔE_p, exceeds the Nernstian requirement of 59 mV expected for a reversible one-electron process. For $Cu(SMML)_2$, this value increases from ΔE_p = 78 mV at 0.05 V/s to ΔE_p = 135 mV at 5 V/s which can be attributed to a kinetic inhibition of the electron transfer process.[69,70] Therefore, the reduction process can be considered to be quasi-reversible. This quasi-reversibility probably arises as a consequence of a geometry change toward a distorted tetrahedral environment around the Cu(I) species.

Antibacterial Activity of the Parent Molecules. In order to select the best complex for further optimization of antibacterial activity, the ligands and complexes of this first series were screened for their antibacterial activity against a panel of four strains of bacteria (Table 3). Since it has been reported that low permeability of the outer membrane[36,37] is a prime factor limiting intracellular activity of potential antimicrobial compounds, the antibacterial tests were also performed in the presence of polymyxin B nonapeptide (PMBN) which is known to permeabilize bacterial membranes for new molecules.[71] In the presence of PMBN, an impressive improvement in biological activity of the tested molecules was observed showing that these compounds did not cross the outer membrane of Gram-negative bacteria efficiently. Therefore, only results obtained in the presence of PMBN will be discussed.

The influence of the efflux pump was assessed by testing the compounds against bacterial strains deleted for certain pump components (*E. coli* AcrAB- and *E. aerogenes* TolC−). The active compounds showed at least 2-fold increase in antibacterial activity toward these strains. In contrast, there was no difference in activity observed for SBML and $Cu(SB4CB)_2$ toward the *E. coli* AcrAB-deleted strains indicating that the compounds were not expelled by this pump. Therefore, the reduction in antibacterial activity of most compounds tested can be primarily attributed to the presence of efflux pumps that similarly affect many antibiotics used clinically.

The free ligands with the aromatic acid substituent exhibited the lowest MIC among the ligands tested. This efficacy may be

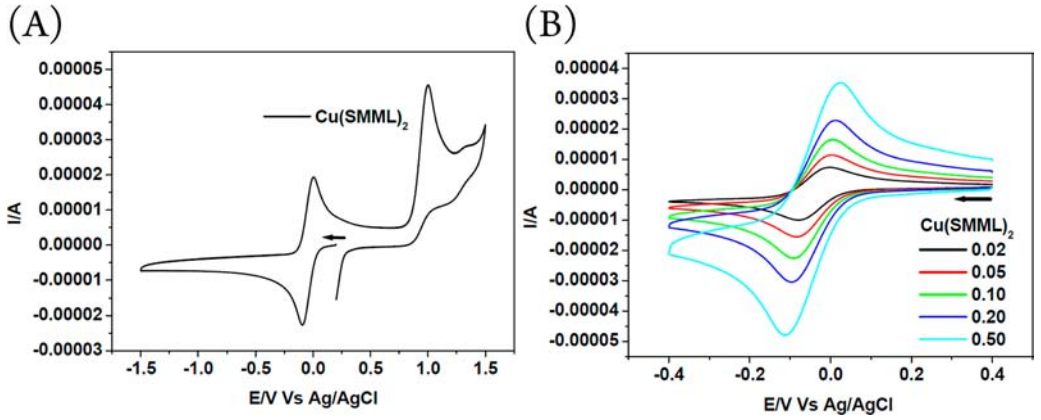

Figure 5. Cyclic voltammograms of the $Cu(SMML)_2$ at 1.7 mM in anhydrous deoxygenated DMF containing 0.1 M tetrabutylammonium perchlorate as the supporting electrolyte at (A) a scan rate of 0.1 V/s and at (B) various scan rates = 0.02, 0.05, 0.1, 0.2, and 0.5 V/s. Working electrode: glassy carbon; counter electrode: Pt wire; reference electrode: Ag/AgCl. All sweeps were initiated in the direction of the arrow.

dx.doi.org/10.1021/bc5004907 | Bioconjugate Chem. 2014, 25, 2269−2284

Table 3. Antimicrobial Activity of Nonconjugated Series

Compound	Minimum Inhibitory Concentration (MIC)[a]			
	E. coli		*E. aerogenes*	
	AG100 WT	AG100A AcrAB-	EA289 AcrAB+	EA298 TolC-
SMML	>128	>128	>128	>128
+ PMBN 1/5	64	32	>128	128-64
$Cu(SMML)_2$	>128	128	>128	>128
+ PMBN 1/5	64	16	>128-128	64 - 16
SMLA	>128	>128	>128	>128
+ PMBN 1/5	64	32	>128	128-64
$Cu(SMLA)_2$	>64	>64	>64	>64
+ PMBN 1/5	64	32	>64	32
SBML	>128	128	>128	>128-128
+ PMBN 1/5	16	16	>128-128	64 - 16
$Cu(SBML)_2$	>128	32-16	>128	>128
+ PMBN 1/5	16	4	>128	4
SBLA	>128	128	>128	128
+ PMBN 1/5	32	8	128	64-16
$Cu(SBLA)_2$	>128	>128	>128	>128
+ PMBN 1/5	32-16	8-4	>128	8
SM4CB	>64	>64	>64	>64
+ PMBN 1/5	>64	>64-32	>64	>64
$Cu(SM4CB)_2$	>64	>64	>64	>64
+ PMBN 1/5	64	32	>64	64
SB4CB	>64	>64-64	>64	>64
+ PMBN 1/5	32	16	>64	16
$Cu(SB4CB)_2$	>64	>64	>64	>64
+ PMBN 1/5	8	8	>64	8-4

[a] μM. Color code: MIC values or average MIC values $\geq$64 μM = red, $\leq$10 μM = green, between 64 μM and 10 μM = colorless. MIC values higher than 64 μM indicate poor antibacterial activity.

the result of increased stability of the compounds due to the presence of the aromatic ring as mentioned earlier. Monitoring of the aromatic Schiff bases (SM4CB and SB4CB) by HPLC and UV−vis spectroscopy showed that they were stable since no hydrolysis was observed even after 24 h.

The activity of most of the compounds was maintained or improved upon complexation with copper. Copper(II) acetate was also screened and was found inactive against all strains (MIC >128 μM) which confirms that the observed growth inhibition was not due to intrinsic biological activity of free copper(II) ions.[72] To characterize the complexation effect independently, the ratio of the MIC of the free ligand to that of the Cu(II) complex (multiplied by 2 due to the coordination of two ligands in a complex) was calculated for the series for each strain (see Supporting Information 6). A ratio greater than 1 reflects a synergistic effect afforded by the complexation (i.e., the activity is not only due to the ligand) whereas a ratio less than one implies that the complexation is deleterious. A majority of the MIC ratios were 1 indicating that complexation did not contribute significantly to the observed activity of the ligands. The activity gain on complexation is highly dependent on the bacterial strain. $Cu(SB4CB)_2$, $Cu(SBML)_2$, and $Cu(SMLA)_2$ showed a positive complexation effect toward *E. coli* WT, *E. coli* AcrAB-, and *E. aerogenes* AcrAB+, respectively. Interestingly, complexation improved the activity for most of compounds with the exception of $Cu(SM4CB)_2$ against the TolC deleted *E. aerogenes* strain. The observed efficiency of the metal complexes could be linked to the significant changes in the physicochemical properties of the compounds upon chelation or/and to their redox properties. There is also a general trend that metal complexes bearing the S-benzyl derived ligands showed better activity than the S-methyl derivatives in this series.

As mentioned earlier, the redox potentials were higher (more positive) for benzyl-substituted compounds with E_{pc} values ranging from −0.066 V to −0.114 V/(AgCl/Ag with Fc^+/Fc = 0.563 V). This could be explained by a weaker electron-donating effect of the benzyl group. Since a higher redox potential means that Cu(II) reduction is easier, consequently a higher content of Cu(I) could be continuously generated due to the reversibility. Considering that Cu(I) is prone to participate in Fenton-type reactions that produce reactive oxygen species (ROS), which can damage biomolecules within cells,[73] the formation of Cu(I) is a possible explanation for the antibacterial activity of these complexes. In the initial part of this study SB4CB was identified as the most promising compound for subsequent conjugation with selected moieties to attempt enhancement of potency.

FUNCTIONALIZED COMPOUNDS

Synthesis. The acid functionality of SB4CB and SM4CB was used to conjugate them with selected vectors comprising cell-penetrating peptides (CPPs), short oligoethylene glycol (OEG), and PAβN, a blocker of resistance-nodulation-division (RND) efflux pumps. The conjugated ligands either were synthesized using solid phase peptide synthesis (SPPS) techniques or were produced in solution. The chosen procedure required optimization for each compound to ensure prevention of hydrolysis and decomposition. The conjugated ligands were synthesized then complexed *in situ* with copper ions to generate the desired copper complexes (Scheme 2).

The Schiff base−OEG conjugate was prepared on solid support using Fmoc strategy with Rink amide resin and standard coupling conditions with HBTU/HOBt. While the Fmoc strategy was relatively straightforward for the OEG conjugate, this synthetic approach was less suitable for polyarginine conjugates. Problems arose because the CPPs were difficult to assemble using Fmoc strategy. Therefore, preparation of the polyarginine peptides was performed using Boc strategy on MBHA resin to obtain C-carboxamide peptides. The CPP couplings were carried out using HBTU/HOBt as coupling reagents when the peptides were synthesized manually and DCC/HOBt when they were synthesized in the synthesizer. The ligands were introduced at the N-terminal amino group of the protected peptidyl resin with HATU/HOAt as efficient coupling agents eliminating the need for repeat coupling. The compounds were removed from the resin with the simultaneous cleavage of the tosyl side-chain protecting groups in HF in the presence of only dimethysulfide (Me_2S) as a radical scavenger since the use of anisole led to an unexpected byproduct. If the conjugates were found to contain formyl-protected tryptophan, the formyl deprotection was subsequently carried out with 20% piperidine in NMP prior to coupling with the Schiff bases to prevent hydrolysis of the Schiff base moiety during the basic treatment. Finally, the conjugation of SB4CB with the efflux pump blocker PAβN was

dx.doi.org/10.1021/bc5004907 | Bioconjugate Chem. 2014, 25, 2269−2284

Scheme 2. Synthetic Pathways for the Functionalized Copper Complexes[a]

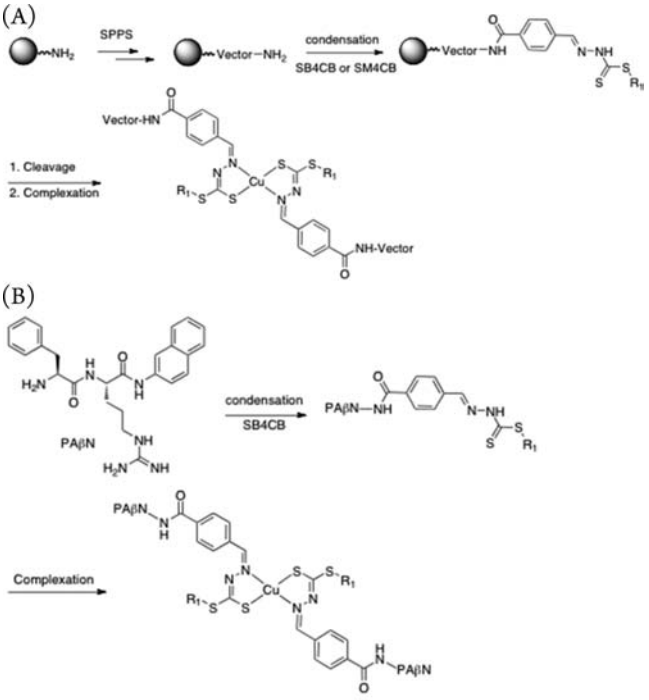

Entry	R_1	Vector	Ligand name	Complex name
7	$-CH_2Ph$	$-(EtO)_2-CH_2CONH_2$	OEG-SB4CB	$Cu(OEG\text{-}SB4CB)_2$
8	$-CH_2Ph$	$-R\text{-}CONH_2$	R1-SB4CB	$Cu(R1\text{-}SB4CB)_2$
9	$-CH_2Ph$	$-R_4\text{-}CONH_2$	R4-SB4CB	$Cu(R4\text{-}SB4CB)_2$
10	$-CH_2Ph$	$-R_9\text{-}CONH_2$	R9-SB4CB	$Cu(R9\text{-}SB4CB)_2$
11	$-CH_2Ph$	$-RW9\text{-}CONH_2$	RW9-SB4CB	$Cu(RW9\text{-}SB4CB)_2$
12	$-CH_2Ph$	-FR-CONH-Naphth.	PAβN-SB4CB	$Cu(PA\beta N\text{-}SB4CB)_2$
13	$-CH_3$	$-R_9\text{-}CONH_2$	R9-SM4CB	$Cu(R9\text{-}SM4CB)_2$
15	$-CH_3$	$-RW9\text{-}CONH_2$	RW9-SM4CB	$Cu(RW9\text{-}SM4CB)_2$

[a](A) On solid support. (B) In solution. R, F, and W are the one-letter nomenclature for amino acids (R = arginine, F = phenylalanine, W = tryptophan). RW9 corresponds to the sequence RRWWRRWRR. Naph is the abbreviation for naphthyl.

effected through solution synthesis using HATU/HOAt in anhydrous DMF. All functionalized ligands were then purified by RP-HPLC, and for each vector, an acetylated version was also synthesized to be used as a control compound for the biological tests. The copper complexes were finally obtained by mixing 0.5 equiv of $Cu(OAc)_2$ with the ligand in MeOH. The expected complexation was monitored by UV−vis spectroscopy and the identification of the complexes was further confirmed by EPR, LC-MS, and ITC.

Characterization of Metal-Complex Conjugates. *UV−vis Spectroscopy.* UV−vis titrations were performed to ascertain the formation of the expected ML_2 complexes. Titrations were carried out in MeOH, which mirrored the actual synthetic procedure and also in acetate buffer at pH 6 for aqueous solution studies.

Upon addition of $Cu(OAc)_2$ to the ligands, changes in UV−vis spectra were observed with the characteristic broad absorption band associated with the complexes formed appearing in the range 300−400 nm with λ_{max} ∼325 nm while the intensity of the band corresponding to ligands at λ_{max} ∼340 nm decreased. For all ligands, the titration performed at a concentration of $\sim 10^{-5}$ M proceeded with a sharp end-point at 0.5 equiv with clear isosbestic points indicative of a single complexation event. Features in this low-energy region of the UV−vis spectrum are the same for the conjugated ligands and the parent compounds, strongly suggesting an identical Cu coordination to the Schiff base in each case ruling out possible coordination to peptide chains of the bioconjugate. Examples of UV−vis titration curves obtained are shown in Figure 6 and Supporting Information 5.6. The identities of all metal complexes were further verified by LC-MS spectrometry and summarized in Supporting Information 5.5.

ITC. ITC experiments were undertaken to determine the thermodynamic parameters for the interaction of selected peptide conjugate ligands with Cu(II) ions during complexation in aqueous solution. The metal ion was titrated into the conjugated ligand. All experiments were run in duplicate or triplicate and the results were corrected for copper dilution. The reactions were endothermic for all the conjugated ligands with ΔH values ranging from 12.2 to 74.4 kJ mol^{-1} (Table 4). The association constants (log K_{ass}) were on the order of ca. 6 with a stoichiometry close to the theoretical value of 0.5. These data strongly support formation of the expected ML_2 complexes in agreement with the UV−vis titrations and show that the vector moiety does not play a crucial role in the complexation event.

EPR. The EPR spectra of the bioconjugated complexes and their parent compounds were very similar in frozen DMF, which is a strong indication that the Cu(II) ion is indeed coordinated to the ligand (SB4CB or SM4CB) in the bioconjugated system rather than unspecifically bound to the vector moiety. Furthermore, the similarity of the EPR parameters of the complexes indicate that conjugation of the C-functionalized Schiff bases with polyarginine and other vectors such as OEG and PAβN has very little effect on its Cu(II) chelating behavior (see Supporting Information 5.7). The EPR spectrum of $Cu(R9\text{-}SB4CB)_2$ was also recorded in acetate buffer at pH 6 (Figure 7). Although the compound showed larger distortion from planarity with increasing f value as compared to the spectra measured in DMF, the f value is still within the square planar range. That the spectrum was different from that of aquated Cu(II) ions in aqueous solution indicates that the ligands remain coordinated to Cu(II) in that environment.

These EPR experiments show that the complexes adopt very similar geometry in solution. However, although the parent complexes showed characteristic one-electron Cu(II)/Cu(I) quasi reversible reduction waves, traces from the complexes $Cu(R1\text{-}SB4CB)_2$, $Cu(OEG\text{-}SB4CB)_2$ and $Cu(PA\beta N\text{-}SB4CB)_2$ did not retain reversibility (Supporting Information 5.8), which may be due to a slow electron transfer.

Antibacterial Activity of Conjugated Compounds. The conjugated ligands and complexes were screened against four bacterial strains in order to select the best candidates for subsequent investigation (Table 5). The antibacterial activity and water solubility of this series were significantly improved with conjugation except in the case of PAβN. This conjugate was initially designed to bypass the effect of efflux pump as well as to probe any synergistic effect with possible new mechanism of action. However, the lack of activity indicated no positive synergy. The OEG and R1 conjugates showed better activity only upon introduction of PMBN. This suggests that the

dx.doi.org/10.1021/bc5004907 | Bioconjugate Chem. 2014, 25, 2269−2284

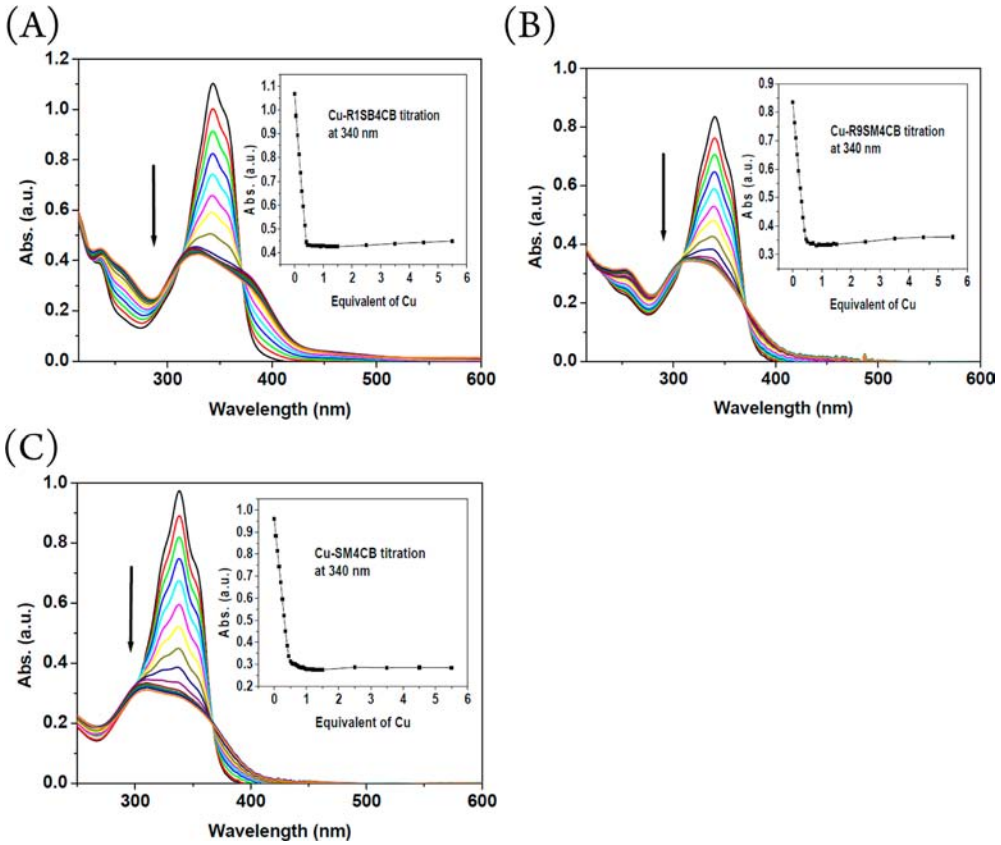

Figure 6. UV−vis titration of various ligands (concentration at ca. 2.5×10^{-5} M) with $Cu(OAc)_2$ (concentration at ca. 5×10^{-4} M) at 25 °C. (A) Titration of R1-SB4CB in methanol and its corresponding titration curve monitored at 340 nm. (B) Titration of R9-SM4CB in acetate buffer pH 6 and its corresponding titration curve monitored at 340 nm. (C) Titration of SM4CB in acetate buffer (pH 6) and its corresponding titration curve monitored at 340 nm.

Table 4. Thermodynamic Parameters of Conjugated Ligand Complexation with Copper Determined by ITC at 25 °C

	log K_{ass}	ΔH^b	n	ΔS^c
$Cu(R1\text{-}SB4CB)_2$	6.00	74.4	0.42	364.5
$Cu(R9\text{-}SM4CB)_2$	6.56	12.2	0.53	166.4
$Cu(R9\text{-}SB4CB)_2$	5.94	24.9	0.49	196.5
$Cu(RW9\text{-}SB4CB)_2$	6.72	60.8	0.55	332.4
$Cu(RW9\text{-}SM4CB)_2$	6.75	36.1	0.43	249.0
$Cu(SB4CB)_2$[a]	5.30	264.6	0.43	984.2

[a]The parent compound is given for the purpose of comparison. [b]kJ mol^{-1}. [c]J mol^{-1} K^{-1}.

addition of a neutral OEG and a single positive charge from R1 were not sufficient to improve the uptake across the membrane of the bacteria. In contrast, R4, R9, and RW9 conjugates were active without the presence of PMBN. The increase in the cationic nature of the polyarginine derivatives allows better interaction and subsequent permeability across the negatively charged bacterial membrane as anticipated.

The OEG, R1, and R4 conjugates also showed at least 2-fold improvement in MIC values against pump deleted strains (*E. coli* AcrAB- and *E. aerogenes* TolC-). However, for R9 and RW9 derivatives, the MIC values remained the same in the presence and absence of active efflux pump. This is another encouraging observation indicating that conjugation to CPP R9 and RW9 is beneficial. In addition to the notable trend with PMBN and efflux pumps, there is also correlation of higher bacterial growth inhibition potency with arginine chain length.

The improvement in the MIC values averaged against all four strains upon conjugation of SB4CB to polyarginine is in the following order: R9-SB4CB > R4-SB4CB > R1-SB4CB > SB4CB. RW9-SB4CB with potentially six positive charges exhibited an average activity in between R9-SB4CB and R4-SB4CB. The number of positive charges seems therefore to play a crucial role. In order to identify the contribution of each moiety, acetylated free peptides and OEG were tested as well. The acetylated vectors OEGAc, R1Ac, and R4Ac were inactive (MIC >128 μM). The improved activity observed for the conjugates of these three vectors could be the result of better water solubility, permeability, and cellular uptake. In contrast, RW9Ac proved to be highly active against all the strains tested, while R9Ac also showed activity against them. As previously mentioned, CPPs and antimicrobial peptides are known to show similar characteristics, in particular, amphiphilicity, which is a crucial factor determining the antibacterial activity of peptides. This seems to be the case for the CPP RW9. Regarding the antimicrobial activity of the acetylated R9Ac and RW9Ac, these two vectors could have contributed to the improved MIC values as demonstrated by the conjugates.

MIC values of most of the bioconjugated Cu(II) complexes were equal to or lower than those for the ligands. The majority of the MIC ratio values calculated were 1 indicating that complexation with Cu(II) did not significantly improve the activity of the ligands. Despite the MIC ratio values, R9 and RW9 conjugates proved to be the most potent derivatives that could escape from the efflux pump and penetrate the cell membrane. In addition, the MIC values of the conjugates were

dx.doi.org/10.1021/bc5004907 | *Bioconjugate Chem.* 2014, 25, 2269−2284

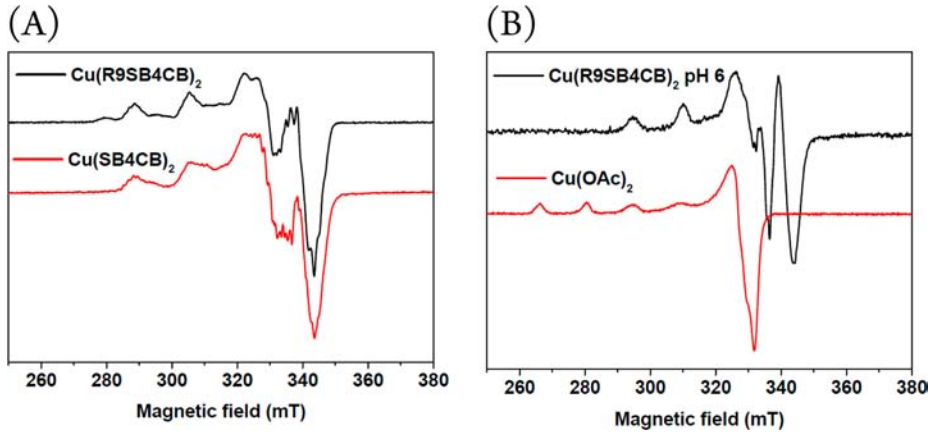

Figure 7. (A) EPR spectra of both parent ($Cu(SB4CB)_2$) and conjugated compounds ($Cu(R9SB4CB)_2$) at 1 mM in frozen DMF. The spectra show that the same species were formed with approximate calculated $g_{\perp}$ and $g_{//}$ values of ∼2.05 and ∼2.15, respectively. (B) EPR spectra of $Cu(R9\text{-}SB4CB)_2$ and $Cu(OAc)_2$ at 1 mM in frozen acetate buffer pH 6 (0.1 M). Microwave frequency = 9.50 GHz, microwave power = 1.00 mW, modulation amplitude = 0.5 mT, modulation frequency = 100 kHz, time constant = 164 ms, temperature = 50 K.

even more effective than standard ciprofloxacin against the *E. aerogenes* strains. It was therefore considered worthwhile to further explore their antibacterial activity by extending the MIC determination to other bacterial species for the conjugates and the acetylated vectors as well as the parent compounds for comparison (Table 6).

The parent compounds SB4CB and $Cu(SB4CB)_2$ were the most active against Gram-positive bacterium *S. aureus* even without the presence of PMBN. Both compounds also showed a wide spectrum of activity against the other Gram-negative bacteria in the presence of PMBN. It is likely that the complexes were more active against the Gram-positive bacterium due to the permeation rate through the membrane as compared to the Gram-negative bacteria. It should be noted that SM4CB, the less active S-methyl analog of SB4CB ligand, was also functionalized with R9 and RW9 in order to better understand the conjugation effect.

The efficacy of the parent compounds against these five bacterial species (as reflected by their MIC values) was considerably increased by modification to form ligand conjugates. Upon conjugation, the functionalized compounds exhibited improved antimicrobial activity with MIC values in the micromolar concentration range, as low as 1−0.5 μM. Further positive results were observed for SM4CB conjugates that were active against most of the bacteria. It is particularly interesting to note the ligand R9-SM4CB is highly active against *S. aureus* with MIC value of 8 μM (without the presence of PMBN) whereas R9Ac (MIC >128 μM) and SM4CB (MIC = 64 μM) were inactive under identical conditions. For comparison with the R9 and RW9 acetylated free peptides, the conjugated ligands were all more active than the acetylated vectors against *A. baumannii*, *P. aeruginosa*, and *S. aureus* without PMBN showing the efficacy of this conjugation. In the presence of the permeabilizing agent PMBN, the trend was the same with the exception of *P. aeruginosa*. Concerning the ligands, the highlight of the MIC results is the high activity against the Gram-positive *S. aureus* in which R9-SB4CB, R9-SM4CB, and RW9-SM4CB all showed better MIC values than their parent ligands, as well as their respective acetylated free peptides.

The complexation effect has been studied using ratio of MIC values with and without PMBN. It is apparent that the complexation is deleterious for RW9 conjugates (most ratios are less than 1). Among the other conjugates, only $Cu(RW9\text{-}SB4CB)_2$ showed a synergy against *P. aeruginosa* without the presence of PMBN. A synergistic effect was also observed for $Cu(R9\text{-}SB4CB)_2$ against *P. aeruginosa*.

It was demonstrated that the EPR properties of the bioconjugates were similar to their parent compounds adopting a square planar geometry in solution. The Cu(II) bioconjugates showed a nonreversible negative shift of the redox couple Cu(II)/Cu(I) potential in the range −0.083 to −0.098 V as compared to $Cu(SB4CB)_2$ at −0.072 V. The loss of reversibility observed herein does not compromise the bioactivity of the compounds $Cu(R1\text{-}SB4CB)_2$ and $Cu(OEG\text{-}SB4CB)_2$, which instead show enhanced antimicrobial efficacy. This suggests the possibility of a different mechanism for the bioconjugates.

CONCLUSION

A new series of open-chain Cu(II) complexes with dithiocarbazate Schiff base chelating ligands has been successfully synthesized and characterized. Although the Schiff bases derived from the keto-ester (methyl levulinate) and keto-acid (levulinic acid and 4-carboxybenzaldehyde) contained O atoms that could potentially participate in coordination, these ligands behaved as bidentate NS ligands coordinating to the central metal through the azomethine nitrogen atom and the thiolate sulfur atom in all complexes. The aromatic ligands were shown to be more stable than the aliphatic ligands and the stability is further improved upon complexation. A series of ligand-bioconjugates was synthesized by either SPPS or solution phase synthesis attesting to the versatility of the ligands SM4CB and SB4CB. The synthetic pathways investigated are robust and can be easily applied to other bioconjugating groups. Cu(II) ion complexation of the bioconjugated ligands was achieved *in situ* and the resulting complexes were studied by a combination of LC-MS, UV−vis, EPR, ITC, and cyclic voltammetry. For the parent complexes, it is clearly evident that antibacterial activities of the compounds are strongly dependent on their substituents and the complexation with copper has a synergetic effect on the activity. The CV scans of the complexes show a Cu(II)/Cu(I) redox quasi-reversibility with a more positive redox potential for the benzyl derivatives than for the methyl derivatives. There is a positive correlation between the antibacterial activity of the complexes and their redox potential. Conjugation of the SB4CB ligand

Table 5. Antibacterial Activity of Conjugated Series

	Minimum Inhibitory Concentration (MIC)[a]			
	E. coli		*E. aerogenes*	
Compound	AG100 WT	AG100A AcrAB-	EA289 AcrAB+	EA298 TolC-
OEGAc	>128	>128	>128	>128
+ PMBN 1/5	>128	>128	>128	>128
OEG-SB4CB	>128	64	>128	>128
+PMBN 1/5	16	8	>128	16
$Cu(OEG\text{-}SB4CB)_2$	>128	>128	>128	>128
+ PMBN 1/5	16	4	>128	8-4
PAβN-SB4CB	>128	>128	>128	>128
+ PMBN 1/5	>128	>128	>128	>128
$Cu(PA\beta N\text{-}SB4CB)_2$	>128	>128	>128	>128
+ PMBN 1/5	>128	>128	>128	>128
R1Ac	>128	>128	>128	>128
+ PMBN 1/5	>128	>128	>128	>128
R1-SB4CB	>128	32	>128-128	128-64
+PMBN 1/5	16	8	128	16
$Cu(R1\text{-}SB4CB)_2$	>128	64	>128	128-64
+ PMBN 1/5	16-8	4	>128	8-4
R4Ac	>128	>128	>128	>128
+ PMBN 1/5	>128	>128	>128	>128
R4-SB4CB	32	16-8	64	16
+PMBN 1/5	16	4	64	8-4
$Cu(R4\text{-}SB4CB)_2$	16-8	8-4	>64-32	8
+ PMBN 1/5	8	2	>64-64	4-2
R9Ac	8	8	8	8
+ PMBN 1/5	4	4	8	8
R9-SB4CB	8	8	8	4
+PMBN 1/5	4	4	4	4
$Cu(R9\text{-}SB4CB)_2$	4	4	4	4
+ PMBN 1/5	2	2	4	2
RW9Ac	2	2	8 - 4	2
+ PMBN 1/5	2	2	4	2
RW9-SB4CB	16 - 4	16	16 - 8	8
+ PMBN 1/5	8	8	8	8
$Cu(RW9\text{-}SB4CB)_2$	8 - 4	8 - 4	16 - 8	8 - 4
+ PMBN 1/5	8	4	8	8
Ciprofloxacin	0.03	0.008	64	32
+ PMBN 1/5	0.015	0.008	64	32

[a] μM. Color code: MIC values or average MIC values ≥64 μM = red, ≤10 μM = green, between 64 μM and 10 μM = colorless. MIC values higher than 64 μM indicate poor antibacterial activity.

Table 6. Antimicrobial Activity Comparison of SB4CB and SM4CB Derivatives

	Minimum Inhibitory Concentration (MIC)[a]				
	Gram -				Gram +
Compound	*A. baumannii* ATCC 19606	*K. pneumoniae* ATCC 11296	*P. aeruginosa* PA01	*S. enterica* SL696	*S. aureus* SA1199
SB4CB	128	>128	>128	>128	16
+ PMBN 1/5	32	32	32	32	8
$Cu(SB4CB)_2$	>128	>128	>128	>128	8 - 4
+ PMBN 1/5	32	>128	64	64	8
SM4CB	>128	>128	>128	>128	64-32
+ PMBN 1/5	64	128	32	>128	64
$Cu(SM4CB)_2$	>128	>128	>128	>128	16
+ PMBN 1/5	>128	>128	128	>128	32
R9Ac	>128	16	>128	64- 6	>128
+ PMBN 1/5	>128	16	>128	8 - 4	64-32
R9-SB4CB	32	32	128 - 64	16	4
+ PMBN 1/5	32	16	128	8	4
$Cu(R9\text{-}SB4CB)_2$	64	32	32	8	2
+ PMBN 1/5	64	16	32	4	1
R9-SM4CB	64	32-6	128	16	8
+ PMBN 1/5	32	16 - 8	>128	4	2
$Cu(R9\text{-}SM4CB)_2$	64	16	64	8	8 - 4
+ PMBN 1/5	64	8	128	4-2	1-0.5
RW9Ac	64-32	16-8	64-32	4 - 2	4
+ PMBN 1/5	128-64	8	4-2	1	2
RW9-SB4CB	32	32	16	8	4
+ PMBN 1/5	32	>16	8	4	2
$Cu(RW9SB4CB)_2$	64-32	32	16	8	4-2
+ PMBN 1/5	32	>16	8	4	1
RW9-SM4CB	8	16-8	16	4-2	2-1
+ PMBN 1/5	16	16	16-8	2-1	1
$Cu(RW9SM4CB)_2$	16-8	16-8	16	2-1	1
+ PMBN 1/5	16	16	8	1	1-0.5
Ciprofloxacin	2	0.25	0.5-0.25	0.03	1
+ PMBN 1/5	2	0.125	-	0.03	1-0.5

[a] μM. Color code: MIC values or average MIC values ≥64 μM = red, ≤10 μM = green, between 64 μM and 10 μM = colorless. MIC values higher than 64 μM indicate poor antibacterial activity.

with the efflux pump blocker PAβN does not enhance antimicrobial activity. However, SB4CB conjugation with positively charged peptides leads to significantly improved bioactivity, which increases with the degree of positive charge within the vector moiety. With the CPPs R9 and RW9, no permeabilizing agent is required and the activity is not affected by the activity of the AcrAB-TolC efflux pumps. For these conjugates, depending on the strain, the antibacterial activity is either governed by the peptide itself or is the result of a synergetic effect upon conjugation. The conjugates are active against a wide range of bacteria and more particularly toward the Gram-positive *S. aureus*. In most cases formation of the

dx.doi.org/10.1021/bc5004907 | *Bioconjugate Chem.* 2014, 25, 2269−2284

complexes does not enhance the efficacy of the ligands except for R9 conjugates against *S. aureus* and *P. aeruginosa*. In contrast to the parent complexes, the Cu(II)/Cu(I) redox wave of the conjugated complexes is not reversible. Consequently, the antibacterial activity of the bioconjugated complexes may not involve the formation of Cu(I) which is prone to participate in Fenton-type reactions that produce reactive oxygen species that can damage biomolecules within bacteria. The mechanism of action of these complexes is still not understood, but this pioneering conjugation with dithiocarbazate ligands demonstrated the utility of the combination of functionalized dithiocarbazate derivatives with various vectors to generate bioconjugates with enhanced antimicrobial activity, membrane permeability and water solubility.

MATERIALS AND METHODS

Synthesis. *Preparation of Parent Ligands.* The general procedure used to prepare the ligands is summarized as follows: to a solution of S-substituted dithiocarbazate in the solvent indicated (see Supporting Information 3), an equimolar amount of levulinic acid/methyl levulinate/4-carboxybenzaldehyde in the same solvent was added dropwise. The mixture was heated to reduce the volume to about 1/3 of the original volume and then placed in the refrigerator overnight. The products were filtered, washed with diethyl ether and dried *in vacuo* over silica gel. Each compound was recrystallized from the solvent used for its synthesis and crystals suitable for X-ray diffraction analysis were obtained from the same solvent through slow evaporation at room temperature. The purity of the products and their stability when dissolved in the minimum quantity of MeOH/DMSO/water mixture were verified by RP-HPLC.

Preparation of Cu(II) Parent Complexes. To a solution of the ligand in the solvent indicated, a solution containing a half-molar amount of $Cu(OAc)_2 \cdot H_2O$, dissolved in methanol or acetonitrile, was added dropwise. The resulting mixture was stirred overnight at room temperature, concentrated by rotary evaporation, and then let to stand at room temperature. For complexes with SM4CB and SB4CB ligands, the solution was heated to reduce the volume to about 1/3 of the original volume and then let to cool to room temperature or placed in the refrigerator overnight. The products were filtered, washed with pentane, and dried *in vacuo* over silica gel. The purity of the products and their stability when dissolved in the minimum quantity of MeOH/DMSO/water mixture were confirmed by RP-HPLC.

Synthesis on Solid Support Using Fmoc Strategy. The OEG derivative was synthesized on solid support using Fmoc protected MBHA Rink amide resin (loading 0.52 mmol/g). Fmoc removal was performed by using 20% (v:v) piperidine in NMP once for 1 min and then once for 15 min. Coupling of the OEG derivative was achieved using standard coupling conditions: 3 equiv of Fmoc-AEEA−OH, 3 equiv of HBTU and HOBt, and 6 equiv of DIEA in NMP were shaken with the resin for 1 h in a reaction vessel (polypropylene syringe with a frit). Upon completion as determined by Kaiser test monitoring, the Fmoc group of the OEG derivative was removed as previously described. A solution of Schiff base (SB4CB) (3 equiv) with HATU/HOAt (3 equiv/3 equiv) and DIEA (6 equiv) in NMP (1 mL for 0.1 g of resin) was added to the resin. The mixture was allowed to react on the automatic shaker for 2 h. The solution was filtered off, and the resin washed with NMP (3 times), DCM (2 times), and MeOH (2 times), and dried *in vacuo*. Cleavage from the resin was performed by shaking it with a solution of TFA/TIS/H_2O (95:2.5:2.5, v:v:v) for 3 h. The solution was collected and the beads washed with neat TFA (3 times). The volume was reduced by evaporation and cold diethyl ether was added to precipitate the compound, which was then recovered by centrifugation (5 min at 8000 rpm, three times). The crude product was purified with preparative RP-HPLC. For N-terminus acetylated OEG, instead of coupling with the ligand, acetylation was performed with 10% acetic anhydride in DCM for 1 h at room temperature. The compound was cleaved as described, but no precipitation occurred upon addition of diethyl ether. The crude was purified by silica-gel column chromatography.

Synthesis on Solid Support Using Boc Strategy. Side-chain protected peptides (R1, R4, R9, and RW9) were assembled on MBHA resin (loading 0.54 mmol/g) either manually using HBTU/HOBt as coupling agents in basic conditions or using the peptide synthesizer (Applied Biosystem 433A) with DCC/HOBt as coupling agents. Coupling was done as for Fmoc synthesis. All amino acids were coupled as Boc derivatives. The side chain of arginine residues was protected by a tosyl group and that of tryptophan residues was protected by a formyl group. Boc group removal was performed using TFA for 1 min (twice) and followed by washing with 10% DIEA in DCM. The coupling of the Schiff base was achieved as previously described: a solution of Schiff base (SB4CB) (3 equiv) with HATU/HOAt (3 equiv/3 equiv) and DIEA (6 equiv) in NMP (1 mL for 0.1 g of resin) was added to the resin. The mixture was allowed to react on the automatic shaker for 2 h. Deformylation for RW9 was performed sequentially with 20% piperidine in NMP: once for 1, 3, 5, 7, 15, and 30 min and finally once for 60 min. Cleavage from the resin and tosyl protecting group removal were performed using pure HF in the presence of dimethyl sulfide for 2 h at 0 °C. After HF removal, cold diethyl ether was added to precipitate the peptide. The precipitate collected was redissolved using 10% acetic acid in water and freeze−dried. For N-terminus acetylated peptides, the acetylation was performed with 10% acetic anhydride in DCM for 1 h at room temperature.

Synthesis in Solution. The conjugation of SB4CB with PAβN was performed in solution using HATU (1.5 equiv), HOAt (1.5 equiv), and DIEA (5 equiv) in dried DMF. The reaction mixture was stirred overnight at room temperature. Analytical HPLC showed conversion of starting material into a less polar product >50%. After dilution with water, the crude peptide material was purified by HPLC.

Preparation of Cu(II) Complexes with Conjugated Ligands, CuL_2. To the bioconjugated ligand (L) (2 equiv) in methanol was added a solution of $Cu(OAc)_2 \cdot H_2O$ (1 equiv); the solution mixture was stirred overnight and then evaporated to dryness to give brown oily solid.

Bacterial Strains, Culture Media and Chemicals. The bacterial strains chosen for this study are listed in Supporting Information 4. The microorganisms studied included reference (from the American Type Culture Collection) and clinical (Laboratory collection) strains of Gram-negative bacteria *Escherichia coli* (*E. coli*), *Enterobacter aerogenes* (*E. aerogenes*), *Acinetobacter baumannii* (*A. baumannii*), *Klebsiella pneumonia* (*K. pneumonia*), *Pseudomonas aeruginosa* (*P. aeruginosa*), and *Salmonella enterica* (*S. enterica*) serotype Typhimurium as well as Gram-positive *Staphylococcus aureus* (*S. aureus*). EA289 is an *E. aerogenes* KANS (susceptible to kanamycin) MDR isolate

dx.doi.org/10.1021/bc5004907 | *Bioconjugate Chem.* 2014, 25, 2269−2284

that exhibits active efflux of norfloxacin and AcrAB-TolC pumps overproduction, EA298 constructed from EA289 is deleted of TolC[41] AG100 is an *E. coli* Wild Type (WT) and AG100A is its KAN^R (resistant to kanamycin) derivative, deleted of AcrAB and hypersensitive to chloramphenicol, tetracycline, ampicillin, and nalidixic acid.[42] Strains were grown at 37 °C on Mueller-Hinton medium 24 h prior to assay. Mueller-Hinton broth (MHB) was used for the susceptibility test. Polymyxin B nonapeptide (PMBN) was obtained from Sigma-Aldrich and the culture medium was purchased from Becton Dickinson.

Determination of Bacterial Susceptibility. Minimum inhibitory concentration (MIC) is defined as the lowest concentration of compound that inhibits microbial growth of targeted bacteria. The respective MICs were determined using the microdilution method (CLSI). Susceptibilities were determined in 96-well microplates with an inoculum of 2×10^5 cfu in 200 μL of MHB containing 2-fold serial dilutions of samples.[43] MICs were determined in the presence of 0.5% of DMSO. A 200× concentration range of each compound was prepared in DMSO 100% and then diluted with H_2O to obtain a 20× concentration range in DMSO 10%. Then, 10 μL aliquots of these ranges were added to 190 μL of inoculum. The MICs of samples were determined after 18 h incubation at 37 °C, following addition (50 μL) of 0.2 mg/mL iodonitrotetrazolium (INT) and incubation at 37 °C for 30 min. The sample dilution range in this work is 0−128 μM. Samples were tested alone or in the presence of PMBN at 51.2 mg/L final concentration (1/5 of its direct MIC). All assays were performed in duplicate or triplicate. Ciprofloxacin was used as standard antibiotic reference.

■ ASSOCIATED CONTENT

Supporting Information

Detailed experimental and characterization information for all the compounds synthesized; additional spectra, figures and tables for all the characterization; figures on the effect of complexation on the ligands series against the different strains of bacteria. This material is available free of charge via the Internet at http://pubs.acs.org. CCDC 999784−999789 contains the supplementary crystallographic data for this paper. These data can be obtained free of charge from the Cambridge Crystallographic Data Centre at http://www.ccdc.cam.ac.uk/Community/Requestastructure.

■ AUTHOR INFORMATION

Corresponding Authors

*E-mail: kacrouse@gmail.com. Phone: 1 902 322 7473
*E-mail: clotilde.policar@ens.fr. Phone: 33-144322420.
*E-mail: nicolas.delsuc@upmc.fr. Phone: 33-144322447.

Present Address

Karen A. Crouse, Cape Breton University, Sydney, Nova Scotia B1P 6L2, Canada.

Author Contributions

The manuscript was written through contributions of all authors. All authors have given approval to the final version of the manuscript.

Notes

The authors declare no competing financial interest.

■ ACKNOWLEDGMENTS

Support for the project came from French ANR Blanc 2010 METABACT grant, Universiti Putra Malaysia (UPM), the Ministry of Higher Education (Malaysia) and the French Infrastructure for Integrated Structural Biology (FRISBI) ANR-10-INSB-05-01. M. L. Low is grateful for the award of an Erasmus Mundus: Maheva Scholarship and a UPM Graduate Research Fellowship (GRF).

■ ABBREVIATIONS

ACN, acetonitrile; AMPs, antimicrobial peptides; Boc, *tert*-butyloxycarbonyl; CHCA, alpha-cyano-4-hydroxycinnamic acid; CI, chemical ionization; CLSI, Clinical and Laboratory Standards Institute; CPPs, cell-penetrating peptides; CV, cyclic voltammetry; DCC, *N,N′*-dicyclohexylcarbodiimide; DCM, dichloromethane; DIEA, *N,N*-diisopropylethylamine; DMF, dimethylformamide; DMSO, dimethyl sulfoxide; Fmoc-AEEA-OH, [2-[2-(Fmoc-amino)ethoxy]ethoxy]acetic acid; Fmoc, fluorenlymethyloxycarbonyl; HATU, 1-[bis(dimethylamino)-methylene]-1*H*-1,2,3-triazolo[4,5-*b*]pyridinium 3-oxid hexa-fluoro- phosphate; HOBt, hydroxybenzotriazole; HBTU, *N,N,N′,N′*-tetramethyl-O-(1*H*-benzotriazol-1-yl)-uraniumhexafluoro-phosphate; HOAt, 1-hydroxy-7-azabenzo-triazole; INT, iodonitrotetrazolium; KAN^R, resistance to kanamycin; KAN^S, susceptible to kanamycin; MBHA, 4-methylbenzhydrylamine; MDR, multidrug resistance; MHB, Mueller-Hinton broth; MIC, minimum inhibitory concentration; NMP, *N*-methyl-2-pyrrolidone; OEG, oligoethylene glycol; PAβN, phenylalanine-arginine-β-naphthylamide; PBS, phosphate buffered saline; PMBN, polymyxin B nonapeptide; RND, resistance-nodulation-division; SB4CB, 4-(benzylsulfanylthiocarbonyl-hydrazonomethyl)-benzoic acid; SBDTC, *S*-benzyldithiocarbazate; SBLA, 4-(benzylsulfanylthiocarbonyl-hydrazono)-pentanoic acid; SBML, 4-(benzylsulfanylthiocarbonyl-hydrazono)-pentanoic acid methyl ester; SM4CB, 4-(methylsulfanylthiocarbonyl-hydrazonomethyl)-benzoic acid; SMDTC, *S*-methyldithiocarbazate; SMLA, 4-(methylsulfanylthiocarbonyl-hydrazono)-pentanoic acid; SMML, 4-(methylsulfanylthiocarbonyl-hydrazono)-pentanoic acid methyl ester; SPPS, solid phase peptide synthesis; TFA, trifluoroacetic acid; TIS, triisopropylsilane; WT, wild type

■ REFERENCES

(1) Coates, A., Hu, Y., Bax, R., and Page, C. (2002) The future challenges facing the development of new antimicrobial drugs. *Nat. Rev. Drug Discovery 1*, 895−910.

(2) Taubes, G. (2008) The bacteria fight back. *Science 321*, 356−361.

(3) Ali, M. A., Mirza, A. H., Butcher, R. J., Tarafder, M. T. H., Keat, T. B., and Ali, A. M. (2002) Biological activity of palladium(II) and platinum(II) complexes of the acetone Schiff bases of S-methyl- and S-benzyldithiocarbazate and the X-ray crystal structure of the [Pd-(asme)$_2$] (asme=anionic form of the acetone Schiff base of S-methyldithiocarbazate) complex. *J. Inorg. Biochem. 92*, 141−148.

(4) Maurya, M. R., Khurana, S., Azam, A., Zhang, W., and Rehder, D. (2003) Synthesis, characterisation and antiamoebic studies of dioxovanadium(V) complexes containing ONS donor ligands derived from S-benzyldithiocarbazate. *Eur. J. Inorg. Chem. 2003*, 1966−1973.

(5) Maia, P. I. d. S., Fernandes, A. G. d. A., Silva, J. J. N., Andricopulo, A. D., Lemos, S. S., Lang, E. S., Abram, U., and Deflon, V. M. (2010) Dithiocarbazate complexes with the $[M(PPh_3)]^{2+}$ (M= Pd or Pt) moiety: Synthesis, characterization and anti-*Tripanosoma cruzi* activity. *J. Inorg. Biochem. 104*, 1276−1282.

(6) Ravoof, T. B., Crouse, K. A., Tahir, M. I. M., How, F. N., Rosli, R., and Watkins, D. J. (2010) Synthesis, characterization and biological

activities of 3-methylbenzyl 2-(6-methyl pyridin-2-ylmethylene) hydrazine carbodithioate and its transition metal complexes. *Transit. Metal Chem. 35*, 871−876.
(7) How, F. N. F., Crouse, K. A., Tahir, M. I. M., Tarafder, M. T. H., and Cowley, A. R. (2008) Synthesis, characterization and biological studies of S-benzyl-β-N-(benzoyl) dithiocarbazate and its metal complexes. *Polyhedron 27*, 3325−3329.
(8) Duncan, C., and White, A. R. (2012) Copper complexes as therapeutic agents. *Metallomics 4*, 127−138.
(9) Chakraborty, A., Kumar, P., Ghosh, K., and Roy, P. (2010) Evaluation of a Schiff base copper complex compound as potent anticancer molecule with multiple targets of action. *Eur. J. Pharmacol. 647*, 1−12.
(10) Afrasiabi, Z., Sinn, E., Padhye, S., Dutta, S., Padhye, S., Newton, C., Anson, C. E., and Powell, A. K. (2003) Transition metal complexes of phenanthrenequinone thiosemicarbazone as potential anticancer agents: Synthesis, structure, spectroscopy, electrochemistry and in vitro anticancer activity against human breast cancer cell-line, T47D. *J. Inorg. Biochem. 95*, 306−314.
(11) Li, Q.-x., Tang, H.-a., Li, Y.-z., Wang, M., Wang, L.-F., and Xia, C.-G. (2000) Synthesis, characterization, and antibacterial activity of novel Mn(II), Co(II), Ni(II), Cu(II), and Zn(II) complexes with vitamin K3-thiosemicarbazone. *J. Inorg. Biochem. 78*, 167−174.
(12) Joseph, J., Nagashri, K., and Janaki, G. B. (2012) Novel metal based anti-tuberculosis agent: Synthesis, characterization, catalytic and pharmacological activities of copper complexes. *Eur. J. Med. Chem. 49*, 151−163.
(13) Belicchi Ferrari, M., Bisceglie, F., Gasparri Fava, G., Pelosi, G., Tarasconi, P., Albertini, R., and Pinelli, S. (2002) Synthesis, characterization and biological activity of two new polymeric copper(II) complexes with α-ketoglutaric acid thiosemicarbazone. *J. Inorg. Biochem. 89*, 36−44.
(14) Bisceglie, F., Pinelli, S., Alinovi, R., Tarasconi, P., Buschini, A., Mussi, F., Mutti, A., and Pelosi, G. (2012) Copper(II) thiosemicarbazonate molecular modifications modulate apoptotic and oxidative effects on U937 cell line. *J. Inorg. Biochem. 116*, 195−203.
(15) Paterson, B. M., and Donnelly, P. S. (2011) Copper complexes of bis(thiosemicarbazones): From chemotherapeutics to diagnostic and therapeutic radiopharmaceuticals. *Chem. Soc. Rev. 40*, 3005−3018.
(16) Donnelly, P. S. (2011) The role of coordination chemistry in the development of copper and rhenium radiopharmaceuticals. *Dalton Trans. 40*, 999−1010.
(17) Enyedy, É. A., Nagy, N. V., Zsigó, É., Kowol, C. R., Arion, V. B., Keppler, B. K., and Kiss, T. (2010) Comparative solution equilibrium study of the interactions of copper (II), iron (II) and zinc (II) with triapine (3-aminopyridine-2-carbaldehyde thiosemicarbazone) and related ligands. *Eur. J. Inorg. Chem. 2010*, 1717−1728.
(18) Senthil Raja, D., Bhuvanesh, N. S., and Natarajan, K. (2011) Biological evaluation of a novel water soluble sulphur bridged binuclear copper (II) thiosemicarbazone complex. *Eur. J. Med. Chem. 46*, 4584−4594.
(19) Stewart, K. M., Horton, K. L., and Kelley, S. O. (2008) Cell-penetrating peptides as delivery vehicles for biology and medicine. *Org. Biomol. Chem. 6*, 2242−2255.
(20) Rijt, S. H. v., Kostrhunova, H., Brabec, V., and Sadler, P. J. (2011) Functionalization of osmium arene anticancer complexes with (poly)arginine: Effect on cellular uptake, internalization, and cytotoxicity. *Bioconjugate Chem. 22*, 218−226.
(21) Cowley, A. R., Dilworth, J. R., Donnelly, P. S., Heslop, J. M., and Ratcliffe, S. J. (2007) Bifunctional chelators for copper radiopharmaceuticals: The synthesis of [Cu(ATSM)-amino acid] and [Cu(ATSM)-octreotide] conjugates. *Dalton Trans. 2*, 209−217.
(22) Ma, M. T., Cooper, M. S., Paul, R. L., Shaw, K. P., Karas, J. A., Scanlon, D., White, J. M., Blower, P. J., and Donnelly, P. S. (2011) Macrobicyclic cage amine ligands for copper radiopharmaceuticals: A single bivalent cage amine containing two Lys3-bombesin targeting peptides. *Inorg. Chem. 50*, 6701−6710.
(23) Ma, M. T., Neels, O. C., Denoyer, D., Roselt, P., Karas, J. A., Scanlon, D. B., White, J. M., Hicks, R. J., and Donnelly, P. S. (2011) Gallium-68 complex of a macrobicyclic cage amine chelator tethered to two integrin-targeting peptides for diagnostic tumor imaging. *Bioconjugate Chem. 22*, 2093−2103.
(24) Hoyer, J., Schatzschneider, U., Schulz-Siegmund, M., and Neundorf, I. (2012) Dimerization of a cell-penetrating peptide leads to enhanced cellular uptake and drug delivery. *Beilstein J. Org. Chem. 8*, 1788−1797.
(25) Abramkin, S., Valiahdi, S. M., Jakupec, M. A., Galanski, M., Metzler-Nolte, N., and Keppler, B. K. (2012) Solid-phase synthesis of oxaliplatin-TAT peptide bioconjugates. *Dalton Trans. 41*, 3001−3005.
(26) Riley, T., and Riggs-Sauthier, J. (2008) The benefits and challenges of PEGylating small molecules. *Pharm. Technol. 32*, 88−94.
(27) Veronese, F. M., and Pasut, G. (2005) PEGylation, successful approach to drug delivery. *Drug Discovery Today 10*, 1451−1458.
(28) Vives, E. (2005) Present and future of cell-penetrating peptide mediated delivery systems: "Is the Trojan horse too wild to go only to Troy? *J. Controlled Release 109*, 77−85.
(29) Fonseca, S. B., Pereira, M. P., and Kelley, S. O. (2009) Recent advances in the use of cell-penetrating peptides for medical and biological applications. *Adv. Drug Delivery Rev. 61*, 953−964.
(30) Regberg, J., Srimanee, A., and Langel, Ü. (2012) Applications of cell-penetrating peptides for tumor targeting and future cancer therapies. *Pharmaceuticals 5*, 991−1007.
(31) Wender, P. A., Mitchell, D. J., Pattabiraman, K., Pelkey, E. T., Steinman, L., and Rothbard, J. B. (2000) The design, synthesis, and evaluation of molecules that enable or enhance cellular uptake: Peptoid molecular transporters. *Proc. Natl. Acad. Sci. U. S. A. 97*, 13003−13008.
(32) Strøm, M. B., Haug, B. E., Skar, M. L., Stensen, W., Stiberg, T., and Svendsen, J. S. (2003) The pharmacophore of short cationic antibacterial peptides. *J. Med. Chem. 46*, 1567−1570.
(33) Chantson, J. T., Vittoria Verga Falzacappa, M., Crovella, S., and Metzler-Nolte, N. (2006) Solid-phase synthesis, characterization, and antibacterial activities of metallocene-peptide bioconjugates. *ChemMedChem 1*, 1268−1274.
(34) Pagès, J.-M., Kascakova, S., Maigre, L., Allam, A., Alimi, M., Chevalier, J., Galardon, E., Refregiers, M., and Artaud, I. F. (2013) New peptide-based antimicrobials for tackling drug resistance in bacteria: Single cell fluorescence imaging. *ACS Med. Chem. Lett. 4*, 556−559.
(35) Walrant, A., Correia, I., Jiao, C.-Y., Lequin, O., Bent, E. H., Goasdoué, N., Lacombe, C., Chassaing, G., Sagan, S., and Alves, I. D. (2011) Different membrane behaviour and cellular uptake of three basic arginine-rich peptides. *Biochim. Biophys. Acta 1808*, 382−393.
(36) Pagès, J. M., and Amaral, L. (2009) Mechanisms of drug efflux and strategies to combat them: Challenging the efflux pump of Gram-negative bacteria. *Biochim. Biophys. Acta 1794*, 826−833.
(37) Nikaido, H., Pagès, J.-M. Broad-specificity efflux pumps and their role in multidrug resistance of Gram-negative bacteria. *FEMS Microbiol. Rev. 36*, 340−363.
(38) Pradel, E., and Pagès, J. M. (2002) The AcrAB-TolC efflux pump contributes to multidrug resistance in the nosocomial pathogen *Enterobacter aerogenes*. *Antimicrob. Agents Chemother. 46*, 2640−2643.
(39) Basha, M. T., Chartres, J. D., Pantarat, N., Ali, M. A., Mirza, A. H., Kalinowski, D. S., Richardson, D. R., and Bernhardt, P. V. (2012) Heterocyclic dithiocarbazate iron chelators: Fe coordination chemistry and biological activity. *Dalton Trans. 41*, 6536−6548.
(40) Ali, M. A., Haroon, C. M., Nazimuddin, M., Majumder, S. M. M. u. H., Tarafder, M. T. H., and Khair, M. A. (1992) Synthesis, characterization and biological activities of some new nickel(II), copper(II), zinc(II) and cadmium(II) complexes of quadridentate SNNS ligands. *Transit. Metal Chem. 17*, 133−136.
(41) Zhu, X. H., Liu, S. H., Liu, Y. J., Ma, J., Duan, C. Y., You, X. Z., Tian, Y. P., Xie, F. X., and Ni, S. S. (1998) Syntheses and metal complexes of a quadridentate NNSS ligand derived from S-benzyl dithiocarbazate (H_2L) and crystal structure of the complex of CuL. *Polyhedron 18*, 181−185.
(42) Viveiros, M., Jesus, A., Brito, M., Leandro, C., Martins, M., Ordway, D., Molnar, A. M., Molnar, J., and Amaral, L. (2005)

Inducement and reversal of tetracycline resistance in *Escherichia coli* K-12 and expression of proton gradient-dependent multidrug efflux pump genes. *Antimicrob. Agents Chemother. 49*, 3578−3582.
(43) Kuete, V., Alibert-Franco, S., Eyong, K. O., Ngameni, B., Folefoc, G. N., Nguemeving, J. R., Tangmouo, J. G., Fotso, G. W., Komguem, J., Ouahouo, B. M., Bolla, J. M., Chevalier, J., Ngadjui, B. T., Nkengfack, A. E., and Pagès, J.-M. (2011) Antibacterial activity of some natural products against bacteria expressing a multidrug-resistant phenotype. *Int. J. Antimicrob. Agents 37*, 156−161.
(44) Chan, M.-H. E., Crouse, K. A., Tahir, M. I. M., Rosli, R., Umar-Tsafe, N., and Cowley, A. R. (2008) Synthesis and characterization of cobalt(II), nickel(II), copper(II), zinc(II) and cadmium(II) complexes of benzyl N-[1-(thiophen-2-yl)ethylidene] hydrazine carbodithioate and benzyl N-[1-(thiophen-3-yl)ethylidene] hydrazine carbodithioate and the X-ray crystal structure of bis{benzyl N-[1-(thiophen-2-yl)ethylidene] hydrazine carbodithioate}nickel(II). *Polyhedron 27*, 1141−1149.
(45) Chew, K. B., Tarafder, M. T. H., Crouse, K. A., Ali, A. M., Yamin, B. M., and Fun, H. K. (2004) Synthesis, characterization and bio-activity of metal complexes of bidentate N-S isomeric Schiff bases derived from S-methyldithiocarbazate (SMDTC) and the X-ray structure of the bis[S-methyl-β-N-(2-furyl-methylketone) dithiocarbazato]cadmium(II) complex. *Polyhedron 23*, 1385−1392.
(46) Crouse, K. A., Chew, K.-B., Tarafder, M. T. H., Kasbollah, A., Ali, A. M., Yamin, B. M., and Fun, H. K. (2004) Synthesis, characterization and bio-activity of S-2-picolyldithiocarbazate (S2PDTC), some of its Schiff bases and their Ni(II) complexes and X-ray structure of S-2-picolyl-β-N-(2-acetylpyrrole)dithiocarbazate. *Polyhedron 23*, 161−168.
(47) Ali, M. A., and Tarafdar, M. T. H. (1977) Metal complexes of sulphur and nitrogen-containing ligands: Complexes of S-benzyldithiocarbazate and a Schiff base formed by its condensation with pyridine-2-carboxaldehyde. *J. Inorg. Nucl. Chem. 39*, 1785−1791.
(48) Rapheal, P. F., Manoj, E., and Prathapachandra Kurup, M. R. (2007) Copper(II) complexes of N(4)-substituted thiosemicarbazones derived from pyridine-2-carbaldehyde: Crystal structure of a binuclear complex. *Polyhedron 26*, 818−828.
(49) Belicchi Ferrari, M., Gasparri Fava, G., Pelosi, G., and Tarasconi, P. (2000) Versatile chelating behavior of aliphatic thiosemicarbazones in zinc and cobalt complexes. *Polyhedron 19*, 1895−1901.
(50) Creaven, B. S., Devereux, M., Karcz, D., Kellett, A., McCann, M., Noble, A., and Walsh, M. (2009) Copper (II) complexes of coumarin-derived Schiff bases and their anti-*Candida* activity. *J. Inorg. Biochem. 103*, 1196−1203.
(51) Low, M. L., Ravoof, T. B. S. A., Tahir, M. I. M., Crouse, K. A., and Tiekink, E. R. T. (2013) Pyridin-4-yl)methyl N′-(3-phenylallylidene)hydrazinecarbodithioate. *Acta Crystallogr., Sect. E 69*, o167−o168.
(52) Ravoof, T. B. S. A., Crouse, K. A., Tahir, M. I. M., Cowley, A. R., and Ali, M. A. (2007) Synthesis, characterization and bioactivity of mixed-ligand Cu(II) complexes containing Schiff bases derived from S-benzyldithiocarbazate and saccharinate ligand and the X-ray crystal structure of the copper-saccharinate complex containing S-benzyl-β-N-(acetylpyrid-2-yl)methylenedithiocarbazate. *Polyhedron 26*, 1159−1165.
(53) Manan, M. A. F. A., Crouse, K. A., Tahir, M. I. M., Rosli, R., How, F. N. F., Watkin, D. J., and Slawin, A. M. Z. (2011) Synthesis, characterization and cytotoxic activity of S-benzyldithiocarbazate Schiff bases derived from 5-fluoroisatin, 5-chloroisatin, 5-bromoisatin and their crystal structures. *J. Chem. Crystallogr. 41*, 1630−1641.
(54) Knoblauch, S., Benedix, R., Ecke, M., Gelbrich, T., Sieler, J., Somoza, F., and Hennig, H. (1999) Synthesis, crystal structure, spectroscopy, and theoretical investigations of tetrahedrally distorted copper(II) chelates with $[CuN_2S_2]$ coordination sphere. *Eur. J. Inorg. Chem. 1999*, 1393−1403.
(55) Ali, M. A., Hj Abu Bakar, H. J., Mirza, A. H., Smith, S. J., Gahan, L. R., and Bernhardt, P. V. (2008) Preparation, spectroscopic characterization and X-ray crystal and molecular structures of nickel(II), copper(II) and zinc(II) complexes of the Schiff base formed from isatin and S-methyldithiocarbazate (Hisa-sme). *Polyhedron 27*, 71−79.
(56) Manan, M. A. F. A., Tahir, M. I. M., Crouse, K. A., Rosli, R., How, F. N. F., and Watkin, D. J. (2011) The crystal structure and cytotoxicity of centrosymmetric copper(II) complex derived from S-methyldithiocarbazate with isatin. *J. Chem. Crystallogr. 41*, 1866−1871.
(57) Latheef, L., and Prathapachandra Kurup, M. R. (2008) Spectral and structural studies of nickel (II) complexes of salicylaldehyde 3-azacyclothiosemicarbazones. *Polyhedron 27*, 35−43.
(58) Nair, M. S., and Joseyphus, R. S. (2008) Synthesis and characterization of Co (II), Ni (II), Cu (II) and Zn (II) complexes of tridentate Schiff base derived from vanillin and DL-α-aminobutyric acid. *Spectrochim. Acta, Part A: Mol. Biomol. Spectrosc. 70*, 749−753.
(59) Ali, M. A., Mirza, A. H., and Butcher, R. J. (2001) Synthesis and characterization of copper(II) complexes of the methylpyruvate Schiff base of S-methyldithiocarbazate (Hmpsme) and the X-crystal structures of Hmpsme and [Cu(mpsme)Cl]. *Polyhedron 20*, 1037−1043.
(60) Kivelson, D., and Neiman, R. (2004) ESR studies on the bonding in copper complexes. *J. Chem. Phys. 35*, 149−155.
(61) Chikate, R. C., Belapure, A. R., Padhye, S. B., and West, D. X. (2005) Transition metal quinone-thiosemicarbazone complexes 1: Evaluation of EPR covalency parameters and redox properties of pseudo-square-planar copper (II)-naphthoquinone thiosemicarbazones. *Polyhedron 24*, 889−899.
(62) Diaz, A., Pogni, R., Cao, R., and Basosi, R. (1998) EPR characterization of a series of mono- and bis-thiosemicarbazone copper(II) complexes. *Inorg. Chim. Acta 275*, 552−556.
(63) Krishna, P. M., Reddy, K. H., Pandey, J. P., and Siddavattam, D. (2008) Synthesis, characterization, DNA binding and nuclease activity of binuclear copper (II) complexes of cuminaldehyde thiosemicarbazones. *Transit. Metal Chem. 33*, 661−668.
(64) Chandra, S., and Sangeetika, X. (2004) EPR, magnetic and spectral studies of copper(II) and nickel(II) complexes of schiff base macrocyclic ligand derived from thiosemicarbazide and glyoxal. *Spectrochim. Acta, Part A: Mol. Biomol. Spectrosc. 60*, 147−153.
(65) Beshir, A. B., Guchhait, S. K., Gascon, J. A., and Fenteany, G. (2008) Synthesis and structure-activity relationships of metal-ligand complexes that potently inhibit cell migration. *Bioorg. Med. Chem. Lett. 18*, 498−504.
(66) Blumberg, W., and Peisach, J. (1968) Bis (thiosemicarbazone) and other nitrogen and sulfur ligated complexes of copper (II). *J. Chem. Phys. 49*, 1793−1802.
(67) Da Silva, A. S., De Silva, M. A. A., Carvalho, C. E. M., Antunes, O. A. C., Herrera, J. O. M., Brinn, I. M., and Mangrich, A. S. (1999) Coordination complexes of bifunctional compounds: I. Synthesis and properties of bis [5-(2-oxyphenyl)-3-phenyl-1, 2, 4-oxadiazolyl] copper (II). A fluorescent coordination compound of Cu (II). *Inorg. Chim. Acta 292*, 1−6.
(68) Evans, D. H., O'Connell, K. M., Petersen, R. A., and Kelly, M. J. (1983) Cyclic voltammetry. *J. Chem. Educ. 60*, 290.
(69) dos Santos Claro, P. C., González-Baró, A. C., Parajón-Costa, B. S., and Baran, E. J. (2005) Spectroscopic and electrochemical behavior of the methyl and ethyl derivatives of bis (acetylacetonato) oxovanadium (IV). *Z. Anorg. Allg. Chem. 631*, 1903−1908.
(70) Parajón-Costa, B. S., Wagner, C. C., and Baran, E. J. (2004) Vibrational spectra and electrochemical behavior of bispicolinate copper (II). *J. Arg. Chem. Soc. 92*, 109−117.
(71) Goemaere, E., Melet, A., Larue, V., Lieutaud, A., Alves de Sousa, R., Chevalier, J., Yimga-Djapa, L., Giglione, C., Huguet, F., Alimi, M., Meinnel, T., Dardel, F., Artaud, I., and Pagès, J.-M. (2012) New peptide deformylase inhibitors and cooperative interaction: A combination to improve antibacterial activity. *J. Antimicrob. Chemother. 67*, 1392−1400.
(72) Ng, N. S., Leverett, P., Hibbs, D. E., Yang, Q., Bulanadi, J. C., Jie, W. M., and Aldrich-Wright, J. R. (2013) The antimicrobial properties of some copper(II) and platinum(II) 1,10-phenanthroline complexes. *Dalton Trans. 42*, 3196−3209.

(73) Jansson, P. J., Sharpe, P. C., Bernhardt, P. V., and Richardson, D. R. (2010) Novel thiosemicarbazones of the ApT and DpT series and their copper complexes: Identification of pronounced redox activity and characterization of their antitumor activity. *J. Med. Chem. 53*, 5759−5769.